INDOOR LOCALIZATION AND TRACKING BASED ON RSSI AND ACCELEROMETER MEASUREMENTS

A THESIS SUBMITTED TO
THE GRADUATE SCHOOL OF NATURAL AND APPLIED SCIENCES
OF
MIDDLE EAST TECHNICAL UNIVERSITY

BY

MELIH DOĞAN

IN PARTIAL FULFILLMENT OF THE REQUIREMENTS
FOR
THE DEGREE OF MASTER OF SCIENCE
IN
ELECTRICAL AND ELECTRONICS ENGINEERING

DECEMBER 2015

Approval of the thesis:

INDOOR LOCALIZATION AND TRACKING BASED ON RSSI AND ACCELEROMETER MEASUREMENTS

submitted by **MELIH DOĞAN** in partial fulfillment of the requirements for the degree of **Master of Science in Electrical and Electronics Engineering Department, Middle East Technical University** by,

Prof. Dr. Gülbin Dural Ünver
Dean, Graduate School of **Natural and Applied Sciences** _____

Prof. Dr. Gönül Turhan Sayan
Head of Department, **Electrical and Electronics Engineering** _____

Prof. Dr. Ali Özgür Yılmaz
Supervisor, **Electrical and Electronics Eng. Dept., METU** _____

Assoc. Prof. Dr. Umut Orguner
Co-supervisor, **Electrical and Electronics Eng. Dept., METU** _____

Examining Committee Members:

Prof. Dr. Yalçın Tanık
Electrical and Electronics Engineering Dept., METU _____

Prof. Dr. Ali Özgür Yılmaz
Electrical and Electronics Engineering Dept., METU _____

Assoc. Prof. Dr. Umut Orguner
Electrical and Electronics Engineering Dept., METU _____

Prof. Dr. Çağatay Candan
Electrical and Electronics Engineering Dept., METU _____

Assoc. Prof. Dr. Tolga Girici
Electrical and Electronics Engineering Dept., TOBB ETU _____

Date: _____

I hereby declare that all information in this document has been obtained and presented in accordance with academic rules and ethical conduct. I also declare that, as required by these rules and conduct, I have fully cited and referenced all material and results that are not original to this work.

Name, Last Name: MELIH DOĞAN

Signature :

ABSTRACT

INDOOR LOCALIZATION AND TRACKING BASED ON RSSI AND ACCELEROMETER MEASUREMENTS

Doğan, Melih

M.S., Department of Electrical and Electronics Engineering

Supervisor : Prof. Dr. Ali Özgür Yılmaz

Co-Supervisor : Assoc. Prof. Dr. Umut Orguner

December 2015, 64 pages

In this study, first, received signal strength (RSS) based indoor localization and tracking techniques including maximum likelihood estimation (MLE), Kalman Filter (KF), serial and parallel extended Kalman Filter (EKF) are investigated and their performances compared to each other via a simulation study. Later, sensor fusion with RSS and inertial measurement unit (IMU) for target tracking is discussed to improve accuracy of RSS-based tracking by using KF and EKF as fusion algorithms. Effects of channel parameters and IMU precision to tracking performance are analyzed. Derivations of Posterior Cramer-Rao Bounds for tracking are provided for ONLY RSS and RSS/IMU fusion scenarios with respect to different measurement variances. Finally, we establish a test-bed for RSS based localization and tracking by using Xbee S2 RF modules. ONLY RSS and RSS/IMU fusion scenarios are compared to each other experimentally. RSSI performance is also examined with respect to antenna orientation of Xbee S2 RF module.

Keywords: Kalman Filter, Tracking, RSS, PCRLB, IMU

ÖZ

ALINAN SİNYAL GÜCÜ VE İVMEÖLÇER TABANLI İÇ MEKAN KONUM BULMA VE TAKİP

Doğan, Melih
Yüksek Lisans, Elektrik ve Elektronik Mühendisliği Bölümü
Tez Yöneticisi : Prof. Dr. Ali Özgür Yılmaz
Ortak Tez Yöneticisi : Doç. Dr. Umut Orguner

Aralık 2015 , 64 sayfa

Bu çalışmada ilk olarak, en yüksek benzerlik kestirimi (MLE), Kalman filtresi (KF), seri ve paralel genişletilmiş Kalman filtresi (EKF) içeren, alınan sinyal gücüne (RSS) dayanan iç mekan konumlama ve takipleme teknikleri incelendi ve performansları birbirlerine göre karşılaştırıldı. Daha sonra alınan sinyal gücü (RSS) ve atalet ölçüm ünitesi (IMU) füzyonu kullanılarak RSS tabanlı takipleme doğruluğunun artırılması tartışıldı. Kanal parametrelerinin ve IMU kesinlik değerinin takipleme performansı üzerine etkileri analiz edildi. Sadece RSS ve füzyon senaryoları için sonraki Cramer-Rao alt sınırı farklı ölçüm varyanslarına göre hesaplandı. Son olarak Xbee S2 kablosuz modüllerinden oluşan bir test düzeneği kuruldu. Sadece RSS ve RSS/IMU füzyon senaroları deneysel olarak karşılaştırıldı. Ayrıca almaç oryantasyonuna göre RSS performansı incelendi.

Anahtar Kelimeler: Kalman Filtresi, Takip, Alınan Sinyal Gücü, PCRLB, Atalet Ölçüm Ünitesi

To my family and people who are reading this page

ACKNOWLEDGMENTS

I would like to express my sincere gratitude to my advisor Prof. Dr. Ali Özgür Yılmaz for his guidance, supporting me and for directing me with their valuable feedbacks.

I would like to thank my co-advisor Assoc. Prof. Dr. Umut Orguner for his good advise, patience, inspiring comments and motivations during this thesis.

I am also grateful that I acknowledge the scholarship (2228A) of Scientific and Technological Research Council of Turkey for my master study.

I would like to express my sincere thanks to my colleague and friend Alptekin Yılmaz for having great time working together and sharing experience.

Last but not the least, I would like to express my deepest and warmest gratitude to my parents, Selahattin Doğan and Dilek Doğan, my sister Melike Doğan Ekren, and my friends that are considered as brothers and sisters for believing in, supporting and understanding me during this journey.

TABLE OF CONTENTS

LIST OF TABLES

TABLES

LIST OF FIGURES

FIGURES

LIST OF ABBREVIATIONS

ABBRV	Abbreviation
WSN	Wireless Sensor Networks
GPS	Global Positioning System
TOA	Time of Arrival
AOA	Angle of Arrival
TDOA	Time Difference of Arrival
RSSI	Received Signal Strength Indicator
MLE	Maximum Likelihood Estimation
MDS	Multi Dimensional Scaling
PCRLB	Posterior Cramer Rao Lower Bound
PDF	Probability Density Function
MLE	Maximum Likelihood Estimation
MMSE	Minimum Mean Square Error
EKF	Extended Kalman Filter
UKF	Unscented Kalman Filter
KF	Kalman Filter
CV	Constant Velocity
CA	Constant Acceleration

CHAPTER 1

INTRODUCTION

A Wireless Sensor Network (WSN) is a group of small sensor nodes which are capable of communication, computation and sensing with long life batteries. Recently emerging advanced technologies have made WSNs more feasible with inexpensive nodes. During the past decade, usage of WSNs spread to many areas like energy saving, intelligent buildings and healthcare [2]. Due to these advances in WSN technologies, localization and tracking have become more important because data such as, temperature, humudity coming from nodes without location information is useless most of the time.

In a given WSN, the process of discovering 2D or 3D positions of nodes is referred to as localization. The first thing coming to mind about localization is GPS (Global Positioning System) [3] especially for outdoor environments. In this technology, the travel times of a GPS signal is measured to compute the distances between satellites and a GPS receiver. Due to the obstacles in indoor environments such as walls and furniture, radio wave propagation is affected, in other respects line-of-sight is required for GPS. Also, high cost hardware and high power consumption of GPS can be considered as disadvantages of it. These properties of GPS show that GPS is not feasible for indoor environments. On the other hand, WSNs consist of tiny, low cost, and battery-powered devices that work cooperatively and this have attracted researcher's interest for indoor positioning.

Recently, a great variety of localization techniques based on WSNs that use RF signal measurements have been proposed in literature including time-of-arrival (TOA), angle of arrival (AOA), time difference of arrival (TDOA) and received signal strength

indicator (RSSI) [4, 5]. TOA and TDOA techniques use geometric relationships between anchors and blindfolded nodes but synchronization problems make their application difficult. Also AOA based techniques are unfavorable due to the necessity of antenna arrays. Among these techniques, the popularity of RSS comes from its low complexity and low cost since almost all wireless devices are capable of measuring RSS and reporting it.

Some static localization methods in literature are maximum likelihood estimation (MLE) [6, 7], multidimensional scaling (MDS) [8], trilateration, and multilateration [9, 10]. MLE can be considered to be much more complex, but minimizing estimation error variance with increasing number of measurements and being unbiased makes it conventional, at least as a performance reference. Performances of these RSSI based techniques can be enhanced for tracking moving objects with the Kalman Filter approach which uses prior states and measurements to obtain the trajectory of a moving target. Despite the low complexity of RSS, effects of multi-path channels cause serious errors on the performance of RSS based techniques.

Different type of sensors, absolute and relative sensors, are fused to benefit from each's strengths particularly for low cost devices. One common relative sensor which integrates the accelerometer, gyroscope and magnetometer is Inertial Measurement Unit (IMU) and generally used to increase performance of the GPS-based localization and tracking [11]. Also, there have been research on RSS/IMU fusion for indoor tracking [12, 13].

In this thesis, RSS based indoor localization and tracking are investigated with different algorithms like MLE, Kalman Filter, Serial EKF and Parallel EKF. It is observed that usage of filters bring about remarkable enhancements as compared with static localization, also shown experimentally. Additionally, our main focus is mitigating corresponding errors of RSS based tracking by using RSS/IMU fusion. Rather than a step detection method [14] or using position and velocity information [12, 13], we directly used the raw acceleration data in our fusion case. Tracking by using sensor fusion decreases the error by 30%. Possible effects of channel parameters and IMU measurement precision on tracking performance are also examined. As a system design tool, Posterior Cramer-Rao Lower Bound which is an approach to the bound on

the estimate variance of non-deterministic parameters is studied for indoor RSS based and RSS/IMU fusion tracking problems.

The rest of this study is organized as follows:

In Chapter 2, system models and some localization algorithms in WSNs are defined. In Chapter 3, RSS based indoor tracking concept is investigated in great detail with simulations. PCRLBs are described and calculations for the RSS based systems are introduced in Chapter 4. In Chapter 5, details of the testbed implementation and experimental results are given. Finally, In Chapter 6, by summarizing the study and discussing the future work, we complete the thesis.

CHAPTER 2

SYSTEM MODELS

2.1 Wireless Localization

In WSN localization, usually there are a number of fixed nodes with known coordinates (anchor), some nodes without their location information (blindfolded), and various sensor measurements which are taken between these nodes. These measurements are used to estimate the position of targets as precisely as possible. For the positioning problem, we have to define a model that represents our system.

Suppose a sensor field with *n* blindfolded and *m* anchor nodes with a total of *N=n+m* nodes where *m* anchor nodes (AN) have their positions $a_j = [a_{j1}\ a_{j2}]^T \in \mathbb{R}^2,\ j = 1, ..., m$. The n blindfolded nodes (BN) are at unknown locations $x_i = [x_{i1}\ x_{i2}]^T \in \mathbb{R}^2,\ \ i = 1, ..., n$.

Measurements taken between anchor and blindfolded nodes can be represented as deterministic functions of their positions for different measurement types. Also each measurement has its own measurement errors. The measurement taken between node i and j is shown in 2.1

$$m_{ij} = f(x_i, a_j) + e_{ij} \tag{2.1}$$

where $f(x_i, a_j)$ is a function of positions at x_i and a_j where e_{ij} is the measurement noise. $f(x_i, a_j)$ can be linear or non-linear with respect to positions of nodes. The measurement error e_{ij} can have various characteristics and probability density functions (PDF) depending on the measurement type. In WSN, measurements can be

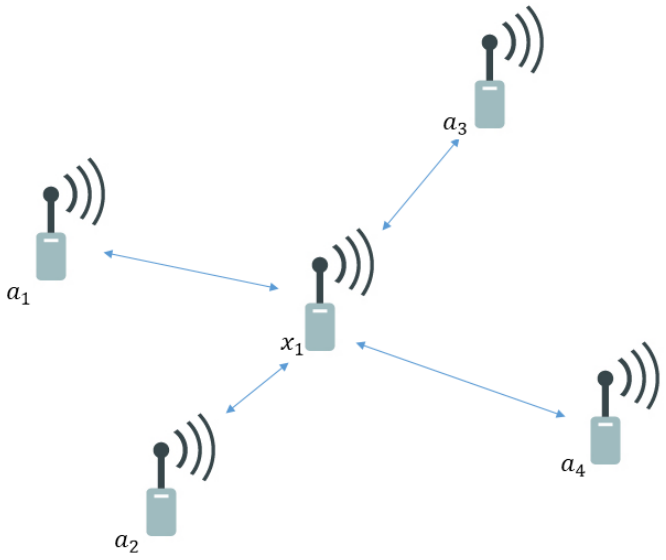

Figure 2.1: A WSN with four anchor node and one blindfolded node

collected at anchors, blindfolded nodes or at both anchor and blindfolded nodes.

2.2 Measurement Types

Since performance of position estimation highly depends on the measurement characteristics, various measurements such as TOA, TDOA, AOA and RSS are used depending on the system requirements. Also accurate measurement models should be used for better performance for localization.

2.2.1 Angle of Arrival (AOA)

The angle between an orientation and a corresponding signal's incoming direction is known as the AOA [15]. The AOA techniques can be examined in two main groups depending on the usage of amplitude response or phase response of the receiver antenna. In the amplitude measuring technique, the direction at which the maximum received signal is measured is considered as the direction of the transmitter. However, a small error on received signal strength can cause large AOA errors. Phase measurement technique requires an antenna array to utilize phase differences at each element of the antenna array to obtain AOA.

Despite the fact that performance of AOA can be enhanced with increasing number of receiver antennas, there are limitations on AOA quality due to shadowing, line-of-sight requirements, and multipath effect. Also, localization using AOA needs antenna array at each node and this increases system complexity and cost [16]. For this reason AOA measurements have not been so far a popular technique for localization problems in WSNs.

2.2.2 Time of Arrival (TOA)

The TOA is propagation time from a transmitter to a receiver and it is used to determine distance between the transmitter and the receiver. To calculate distance, TOA is multiplied with propagation speed which is usually the speed of light denoted by c. Accurate TOA measurements need perfect synchronization between anchors and blindfolded nodes. A TOA measurement can be shown as a circle with its center at transmitter and receiver at some point on the circumference of this circle. At least three transmitters are needed to localize the receiver as given in Figure 2.2 because the position of the receiver is obtained from the intersection of these circles.

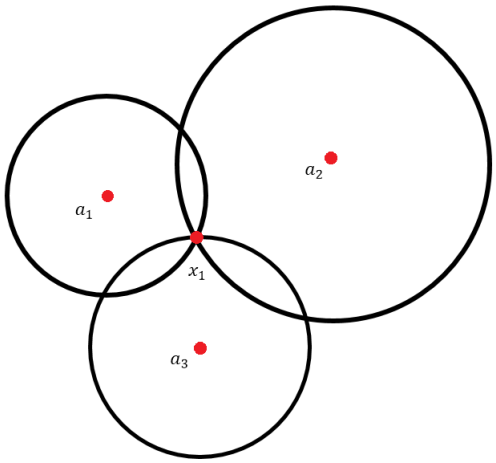

Figure 2.2: Trilateration in 2D space in ideal case

The time difference of arrival (TDOA) based localization is analogous to TOA. Where TOA technique uses propagation time between each anchor and blindfolded node, TDOA uses propagation time differences between each node to localize blindfolded nodes.

Accuracy of TOA techniques may be quite high with perfect synchronization. However this method is sensitive to timing errors in non-line of sight conditions and not robust to multipath effect.

2.2.3 Received Signal Strength Indicator (RSSI)

Received signal strength (RSS) is a popular localization technique because of low cost, easy implementation and low power consumption. All of the lately developed sensor nodes in the market have the ability to measure and deliver RSS without need of extra hardware and this leads us to benefit from savings in cost and power consumption which are essential issues for sensor networks. Our aim in this study is to localize and track a blindfolded node using RSS measurements between anchors and the blindfolded node. To obtain distance from RSS values, we need a propagation model, namely a measurement model. In literature there are different approaches for propagation like Free Space, Log-Normal Shadowing model and ITU Path Loss model [17, 6]. In our study we use Log-Normal Shadowing model. In this model, measured power at receivers RSSI circuit is modeled as follows

$$m_{ij} = \hat{P}_{ij} = P_0 - 10\alpha \log_{10} \frac{\sqrt{(a_{j1} - x_{i1})^2 + (a_{j2} - x_{i2})^2}}{d_0} + e_{ij} = P(d_{ij}) + e_{ij} \quad (2.2)$$

where $\hat{P}_{ij}$ is RSS measurement, $P(d_{ij})$ is received power for an ideal channel, α is path loss exponent, d_0 is reference distance, P_0 is reference power at reference distance d_0 and e_{ij} is a zero-mean Gaussian measurement noise representing the cumulative effects of multipath, shadowing etc. and its variance is σ^2 ($e_{ij} \sim \mathcal{N}(0, \sigma^2)$). Variance σ^2 and path loss exponent α depend on the channel and environment characteristics and they are usually estimated by empirical measurements. Commonly, σ value is between 6dB and 12dB. Considering the channel between nodes i and j, measured RSS from i to j equals to the measured RSS from j to i , i.e., $\hat{P}_{ij} = \hat{P}_{ji}$. The received power can be considered as a random variable with normal distribution where its mean is $P(d_{ij})$ and variance is σ^2 , i.e., $\hat{P}_{ij} \sim \mathcal{N}(P(d_{ij}), \sigma^2)$. Estimating the distance between node i and node j from a given $\hat{P}_{ij}$ can be done by using

Maximum Likelihood Estimation (MLE). In [7], MLE of distance is given as follows

$$\hat{d}_{ij} = 10^{(P_0 - \hat{P}_{ij})/10\alpha} \tag{2.3}$$

where $\hat{d_{ij}}$ is the estimated distance. This estimated distance value can be used directly as a measurement in localization and tracking algorithms.

2.3 Basic Static Localization Algorithms

2.3.1 Maximum Likelihood Estimation

The MLE method is a centralized and well-known approach for localization which could use different measurements like RSS, TOA and connectivity to obtain position estimate [18]. MLE estimators are preferable due to their variance approaching Cramer-Rao lower bound (CRLB) asymptotically [19]. Mainly, in order to estimate the position of a node, MLE minimizes the cost function which consist of differences between measured and estimated distance [4]. In [6], MLE cost function for RSS measurements in a collaborative scenario is given. Also the cost function for TOA and RSS measurements is given in [7]. A conjugate gradient method is often used in order to minimize cost functions of MLE. Assuming all RSS measurements are independent identical distributed (i.i.d.) and all nodes are connected to each other, the MLE cost function of a configuration matrix of blindfolded nodes in 2D for RSS measurement is written as follows [6]

$$MLE_{RSS}(X) = \sum_{i=1}^{n} \sum_{j=i+1}^{N} (\log(d_{ij}) - \log(\hat{d_{ij}}))^2 \tag{2.4}$$

where configuration matrix $X = [x_1\ x_2\ ...\ x_n\ a_{n+1}\ a_{n+2}...\ a_N]^T$, $x_i = [x_{i1}\ x_{i2}]^T$, $a_j = [a_{j1}\ a_{j2}]^T$ carries locations of nodes, n represents the number of the BNs and number of all nodes is $n + m$ equals to N. As mentioned previously, gradient based algorithms are commonly used to minimize MLE cost function. One problem of such algorithms is that there are locally optimal solutions besides the global optimal solution. Because of this problem, MLE is sensitive to initial estimate when run with

the aforementioned algorithms. In order to overcome this situation, initial values should be set carefully or estimated by another estimation method.

2.3.2 Multidimensional Scaling Algorithms

Multidimensional Scaling (MDS) is a statistical technique used to analyze distance-like data in multidimensional space and displays structure of data as a geometrical picture [20]. MDS applications are commonly used in a great variety of areas, such as psychology, statistics, visualization, marketing and so on. MDS technique usage is also popular in localization problems [21, 6, 22, 23]. Given configuration matrix $X = [x_1\ x_2\ ...\ x_n\ a_{n+1}\ a_{n+2}...\ a_N]^T$, calculation of MDS in 2D is made by minimizing the $stress$ given in [20]

$$MDS_{RSS}(X) = \sum_{i=1}^{N-1} \sum_{j=i+1}^{N} (d_{ij} - \hat{d_{ij}})^2 \tag{2.5}$$

where d_{ij} is the euclidean distance between nodes i and j (either blindfolded or anchor) and measured distance is $\hat{d}_{ij}$. This minimization problem typically can be solved with SMACOF (Scaling by MAjorizing a COmplicated Function) [24] or gradient based approaches [20].

In literature, several enhanced and hybrid MDS algorithms have been proposed recently. In [22] and [6] integrated MDS-MLE method is proposed to benefit from different advantages of both MLE and MDS. In this method, firstly, an estimate is obtained from MDS in order to use advantage of superior convergence of it and afterwards MLE is used for tuning MDS results to remove modeling errors caused by MDS method. Throughout the simulations it is shown that a MDS-MLE method has better performance than both MDS and MLE [22]. In [8] a classic MDS algorithm based MDS-MAP method is proposed by Shang. In MDS-MAP, shortest paths from each node to another are computed in order to form a distance matrix. After applying MDS to this matrix, absolute coordinates are obtained with sufficiently many number of anchors (3 or 4) through a linear transformation.

2.3.3 Trilateration and Multilateration

Trilateration is the process of obtaining the position of a node from its distance to three anchors. Three circles are formed based on these distance measurements and intersection of them is used to localize the node in space [25]. The centers of these circles are at anchor locations and distance measurements from the anchor to blindfolded node determine the circle radius. The trilateration scheme is shown in Figure 2.2 and more information about trilateration is given in [9]. Being easy to implement makes trilateration quite popular with various measurement types, such as RSS, TOA and TDOA, but errors are inevitable for each of them. Despite the fact that trilateration gives accurate results with low-noise distance measurements, it is not feasible with high-noise measurement errors or with collinearity of three anchors.

When three anchors do not produce sufficiently good localization results, a possible solution is using measurements from multiple neighbor nodes, which is called multilateration [25]. As described in [3], GPS is an example of localization that is based on TDOA measurements and multilateration. Usually intersection of distance measurements is not a single point and obtaining position of a node is posed as a Least Square Estimation (LSE) problem.

In the literature, there are several different approaches based on multilateration. In [10] a collaborative multilateration algorithm is suggested which facilitates estimation of node locations in multi-hop sensor deployments by known anchor locations and distance measurements. With this algorithm, localization of blindfolded nodes which cannot communicate directly with anchors is possible. Also collaborative multilateration and iterative multilateration for ad-hoc node deployment is proposed in [26]. Iterative multilateration is a distributed algorithm and all nodes in the network is capable of running it.

CHAPTER 3

TRACKING ALGORITHMS

3.1 Problem Statement

Object/target tracking represents a problem to estimate location, trajectory and characteristics of an object by using sensor measurements and kinematic models [27]. The measurements consist of all information about the object in the environment reported from the sensor which can be any measuring device like camera, smart phone, radar, or other tiny devices. The typical tracking problem is actually a state estimation problem where the state is composed of kinematic variables like position, velocity and the acceleration. There are various well-known Bayesian tracking algorithms namely filters in literature [28, 29, 30] and most common ones are Kalman filter and its extensions. We consider the state space model below

$$x_k = f(x_{k-1}) + w_k \tag{3.1}$$

$$y_k = h(x_k) + v_k \tag{3.2}$$

where

- $x_k \in \mathbb{R}^{n_x}$ is the state with the initial state $x_0 \sim p(x_0)$;
- $y_k \in \mathbb{R}^{n_y}$ is the observation;
- $w_k \in \mathbb{R}^{x_n}$ is a process noise and its distribution $p(w_k)$ independent from x_k;
- $v_k \in \mathbb{R}^{y_n}$ is the white measurement noise with a known distribution $p(v_k)$ inde-

pendent from x_k.

Finding the posterior density $p(x_k|y_{1:k})$ is a main goal in Bayesian state estimation, $y_{1:k} \triangleq \{y_1, y_2, ...y_k\}$ represents the measurement sequence. The process noise w_k is introduced to account for unknown disturbance on the system dynamics. In other words, a larger process noise represents that we trust less on the state equation. Similarly the measurement noise v_k is introduced to account for imperfections in measured data. There are basic equations namely prediction and update for computing posterior density from previous state's recursively. This recursive solution is derived from Total Probability Law and Bayes Theorem [31] as follows

$$p(x_{k-1}|y_{1:k-1}) \xrightarrow{prediction} p(x_k|y_{1:k-1}) \xrightarrow{update} p(x_k|y_{1:k}) \tag{3.3}$$

For each k starting with $p(x_0)$ and $k = 1$;

- Prediction update

$$p(x_k|y_{1:k-1}) = \int p(x_k|x_{k-1})p(x_{k-1}|y_{1:k-1})dx_{k-1} \tag{3.4}$$

- Measurement update

$$p(x_k|y_{1:k}) = \frac{p(y_k|x_k)p(x_k|y_{1:k-1})}{p(y_k|y_{1:k-1})} \tag{3.5}$$

where

$$p(y_k|y_{1:k-1}) = \int p(y_k|x_k)p(x_k|y_{1:k-1})dx_k. \tag{3.6}$$

With the knowledge of $p(x_k|y_{1:k})$, it is possible to obtain an optimal estimate according to a suitable benchmark. The most common one is the minimum mean square error (MMSE) and the estimates for the predicted and estimated states are given as

$$\begin{aligned} \hat{x}_{k|k-1}^{MMSE} &= E[x_k|y_{1:k-1}], \\ \hat{x}_{k|k}^{MMSE} &= E[x_k|y_{1:k}]. \end{aligned} \tag{3.7}$$

3.2 Kinematic Models For Target Tracking

3.2.1 (Nearly) Constant Velocity Model

Considering the motion in two dimension (2D), the most common motion is the no motion $x_{k+1} = x_k$. For the moving objects the simplest motion is the motion with a constant velocity (CV). The state of CV model composed of the velocity and position of the moving object is as follows

$$X_k^{CV} = [x_k \ \dot{x}_k \ y_k \ \dot{y}_k]^T \tag{3.8}$$

where x_k and $\dot{x_k}$ represent position and velocity of target on the x-axis, y_k and $\dot{y_k}$ are also for the y-axis. The general state model is given as,

$$X_k^{CV} \triangleq \begin{bmatrix} x_k \\ \dot{x}_k \\ y_k \\ \dot{y}_k \end{bmatrix} = \begin{bmatrix} 1 & T & 0 & 0 \\ 0 & 1 & 0 & 0 \\ 0 & 0 & 1 & T \\ 0 & 0 & 0 & 1 \end{bmatrix} \begin{bmatrix} x_{k-1} \\ \dot{x}_{k-1} \\ y_{k-1} \\ \dot{y}_{k-1} \end{bmatrix} + \begin{bmatrix} T^2/2 & 0 \\ T & 0 \\ 0 & T^2/2 \\ 0 & T \end{bmatrix} \begin{bmatrix} a_k^x \\ a_k^y \end{bmatrix} \tag{3.9}$$

where $a_k^x \sim \mathcal{N}(0, {\sigma_a}^2)$ and $a_k^y \sim \mathcal{N}(0, {\sigma_a}^2)$ represent the change in velocity (acceleration) that is considered as a Gaussian. The reason of saying "nearly" while describing this model is the fluctuation on velocity which is acceleration is assumed to be Gaussian white noise.

3.2.2 (Nearly) Constant Acceleration Model

In this model, target position, velocity and acceleration form the state vector given as

$$X_k^{CA} = [x_k \ \dot{x}_k \ \ddot{x}_k \ y_k \ \dot{y}_k \ \ddot{y}_k]^T \tag{3.10}$$

where $\ddot{x}_k$ and $\ddot{y}_k$ are the accelerations on the x and y-axis. The reason of saying "nearly" while describing this model is the fluctuation on acceleration which is as-

sumed to be Gaussian white noise. The state space model for this model is as follows,

$$X_k^{CA} \triangleq \begin{bmatrix} x_k \\ \dot{x}_k \\ \ddot{x}_k \\ y_k \\ \dot{y}_k \\ \ddot{y}_k \end{bmatrix} = \begin{bmatrix} 1 & T & T^2/2 & 0 & 0 & 0 \\ 0 & 1 & T & 0 & 0 & 0 \\ 0 & 0 & 1 & 0 & 0 & 0 \\ 0 & 0 & 0 & 1 & T & T^2/2 \\ 0 & 0 & 0 & 0 & 1 & T \\ 0 & 0 & 0 & 0 & 0 & 1 \end{bmatrix} \begin{bmatrix} x_{k-1} \\ \dot{x}_{k-1} \\ \ddot{x}_{k-1} \\ y_{k-1} \\ \dot{y}_{k-1} \\ \ddot{y}_{k-1} \end{bmatrix} + \begin{bmatrix} T^2/2 & 0 \\ T & 0 \\ 1 & 0 \\ 0 & T^2/2 \\ 0 & T \\ 0 & 1 \end{bmatrix} \begin{bmatrix} n_k^x \\ n_k^y \end{bmatrix} \tag{3.11}$$

where $n_k^x \sim \mathcal{N}(0, {\sigma_n}^2)$ and $n_k^y \sim \mathcal{N}(0, {\sigma_n}^2)$ are white noises.

3.3 Kalman Filters

The Kalman filter (KF) is proposed by R.E. Kalman as a novel recursive solution to the linear filtering problem in 1960 [32]. Thenceforward, KF has drawn interest from extensive research areas with the advances in digital computing. The explanatory information of the KF is given in first chapter of [33].

Basically, the Kalman filter consists of mathematical equations that form a predictor-corrector type estimator. Kalman filter is optimal in the sense of minimizing mean square error with the assumptions of independent Gaussian noise and linearity of the model. The key point of this optimality is that Kalman filter fuses all available information. All noisy measurements, system and measurement device dynamics, statistics of noises, measurement errors, ambiguity of dynamic models, and knowledge about initial conditions are incorporated in Kalman filter [33]. Since it is a recursive algorithm, KF does not need to keep previous data in storage and the filtering process is repeated when a new measurement is available. There are some variants of KF in the literature and most prevalents are the Extended KF [34, 28] and unscented KF [35, 36]. These are widespread algorithms in the field of data processing.

3.3.1 Kalman Filter

The most special case of the state space system given in Section (3.1) is a linear Gaussian system. In this case we consider the linear system below

$$\begin{aligned} x_k &= Ax_{k-1} + w_k \\ y_k &= Hx_k + v_k \end{aligned} \tag{3.12}$$

with the $process$ noise w_k and $measurement$ noise v_k terms. These are Gaussian and have probability distributions as follows

$$\begin{aligned} w_k &\sim \mathcal{N}(0, Q) \quad where \quad Q > 0 \in \mathbb{R}^{n_x \times n_x} \\ v_k &\sim \mathcal{N}(0, R) \quad where \quad R > 0 \in \mathbb{R}^{n_y \times n_y}. \end{aligned} \tag{3.13}$$

where Q and R $process\ noise\ covariance$ and $measurement\ noise\ covariance$ respectively. For this special case, all posterior densities are Gaussian. The KF algorithm is based on feedback control; begin with the estimation of the process from the state space model, after that noisy measurements are used to give a feedback to the filter. Hence, the algorithm can be examined in two main parts $prediction\ update$ and $measurement\ update$. As a result, this algorithm represents a predictor-corrector type estimation problem. Recursive process flow taken from [1] is given in Table 3.1 and the terms in this algorithm are named in the literature as follows.

- $\hat{x}_{k|k-1}$: Predicted State
- $P_{k|k-1}$: A priori estimate covariance
- $\hat{x}_{k|k}$: A posteriori state estimate
- $P_{k|k}$: Estimate covariance
- $\hat{y}_{k|l-1}$: Predicted measurement
- $(y_k - \hat{y}_{k|k-1})$:Measurement residual (innovation)
- $S_{k|k-1}$: Covariance of predicted measurement (Residual covariance)
- K_k: Kalman gain

TABLE 3.1: *Kalman Filter [1]*

- Initialization with $\hat{x}_{0|0}$, $P_{0|0}$ and $k = 1$
- For each k

  - Prediction Update

    $$\hat{x}_{k|k-1} = A\hat{x}_{k-1|k-1}$$
    $$P_{k|k-1} = AP_{k-1|k-1}A^T + Q$$

  - Measurement Update

    $$\hat{x}_{k|k} = \hat{x}_{k|k-1} + K_k(y_k - \hat{y}_{k|k-1})$$
    $$P_{k|k} = P_{k|k-1} - K_k S_{k|k-1} K_k^T$$

    where

    $$\hat{y}_{k|k-1} = H\hat{x}_{k|k-1}$$
    $$S_{k|k-1} = HP_{k|k-1}H^T + R$$
    $$K_k = P_{k|k-1}H^T S_{k|k-1}^{-1}$$

The KF propagates the conditional probability density shown in (3.3) and calculates the state estimate by minimizing mean square error. Under the linearity and Gaussian assumptions, since the pdf $p(x_k|y_{1:k})$ is Gaussian, it is sufficient to propagate only mean $\hat{x}_{k|k}$ and covariance $P_{k|k}$ as shown in 3.14.

$$\hat{x}_{k-1|k-1}, P_{k-1|k-1} \xrightarrow{prediction} \hat{x}_{k|k-1}, P_{k|k-1} \xrightarrow{update} \hat{x}_{k|k}, P_{k|k} \tag{3.14}$$

3.3.2 Extended Kalman Filter

In most filtering problems, system dynamics are not linear and conditional probability densities are non-Gaussian. In searching the optimum solution for the nonlinear filtering problem, we need conditional probability density functions but infinitely many parameters are required for an exact description. For this reason, some approximations are proposed in the literature [37, 38, 39].

The most common and basic approach for nonlinear filtering is the linearization which is used in Extended Kalman Filter (EKF). In EKF, all non-linear models are linearized

to apply the original Kalman filter equations. Consider the non-linear system below,

$$\begin{aligned} x_k &= f(x_{k-1}) + w_k \\ y_k &= h(x_k) + v_k \end{aligned} \tag{3.15}$$

with process noises $w_k \sim \mathcal{N}(0, Q)$, measurement $v_k \sim \mathcal{N}(0, R)$ and initial state $p(x_0) \sim \mathcal{N}(x_0, P_{0|0})$. Recursive algorithm of EKF is given in Table 3.2

TABLE 3.2: *Extended Kalman Filter [1]*

- Initialization with $\hat{x}_{0|0}$, $P_{0|0}$ and $k = 1$
- For each k

  - Prediction Update

    $$\hat{x}_{k|k-1} = f(\hat{x}_{k-1|k-1})$$
    $$P_{k|k-1} = F P_{k-1|k-1} F^T + Q$$

    where

    $$F = \frac{\partial f}{\partial x_{k|k-1}}|_{x_{k-1}=\hat{x}_{k-1|k-1}}$$

  - Measurement Update

    $$\hat{x}_{k|k} = \hat{x}_{k|k-1} + K_k(y_k - \hat{y}_{k|k-1})$$
    $$P_{k|k} = P_{k|k-1} - K_k S_{k|k-1} K_k^T$$

    where

    $$\hat{y}_{k|k-1} = h(\hat{x}_{k|k-1})$$
    $$H = \frac{\partial h}{\partial x_k}|_{x_k=\hat{x}_{k|k-1}}$$
    $$S_{k|k-1} = H P_{k|k-1} H^T + R$$
    $$K_k = P_{k|k-1} H^T S_{k|k-1}^{-1}$$

The matrices F and H are $Jacobian$ matrices of the non-linear functions. One of the drawbacks of EKF is that EKF can be highly unstable when there is high uncertainty in the variable to be transformed. Also, in some applications $Jacobian$ matrices are very complex and can make the implementation of the filter difficult [40]. On the other hand, EKF can give good results with small uncertainty.

In case of more than one measurement source and high-dimensional measurements, processing the measurements serially prevents the high dimensional matrix inversions in the measurement update part. Hence we can talk about two versions of EKF which

are Serial EKF and Parallel EKF and they differ from each other in the way they process measurements. Serial EKF algorithm is given Table 3.3 and Parallel EKF is given in Table 3.4

TABLE 3.3: *Serial EKF*

- Initialization with $\hat{x}_{0|0}$, $P_{0|0}$ and $k = 1$
- For each k

  - Prediction Update

    $\hat{x}_{k|k-1} = f(\hat{x}_{k-1|k-1})$

    $P_{k|k-1} = FP_{k-1|k-1}F^T + Q$

    where

    $F = \frac{\partial f}{\partial x_{k|k-1}}|_{x_{k-1}=\hat{x}_{k-1|k-1}}$

  - Sort the measurements such that $y_k = [y_{max}...y_{min}]$

  - Set j=1, **for each** $j \leq N$

    - Measurement Update

      $\hat{x}_{k|k-1} = \hat{x}_{k|k-1} + K_k(y_{k,j} - \hat{y}_{k|k-1})$

      $P_{k|k-1} = P_{k|k-1} - K_k S_{k|k-1} K_k^T$

      where

      $\hat{y}_{k|k-1} = h_j(\hat{x}_{k|k-1})$

      $H_j = \frac{\partial h_j}{\partial x_k}|_{x_k=\hat{x}_{k|k-1}}$ (H_j is $Jacobian$ matrix for the measurement source j with measurement $y_{k,j}$)

      $S_{k|k-1} = H_j P_{k|k-1} {H_j}^T + R$

      $K_k = P_{k|k-1} {H_j}^T S_{k|k-1}^{-1}$

      end for

      $\hat{x}_{k|k} = x_{k|k-1}$

      $P_{k|k} = P_{k|k-1}$

TABLE 3.4: *Parallel EKF*

- Initialization with $\hat{x}_{0|0}$, $P_{0|0}$ and $k = 1$
- For each k

  - Prediction Update

    $$\hat{x}_{k|k-1} = f(\hat{x}_{k-1|k-1})$$
    $$P_{k|k-1} = FP_{k-1|k-1}F^T + Q$$

    where

    $$F = \frac{\partial f}{\partial x_{k|k-1}}|_{x_{k-1}=\hat{x}_{k-1|k-1}}$$

  - $h = [h_1 h_2 ... h_N]^T$ for N number of measurement
  - $y_k = [y_1 y_2 ... y_N]^T$: measurement vector
  - Measurement Update

    $$\hat{x}_{k|k} = \hat{x}_{k|k-1} + K_k(y_k - \hat{y}_{k|k-1})$$
    $$P_{k|k} = P_{k|k-1} - K_k S_{k|k-1} K_k^T$$

    where

    $$\hat{y}_{k|k-1} = h(\hat{x}_{k|k-1})$$
    $$H = \frac{\partial h}{\partial x_k}|_{x_k=\hat{x}_{k|k-1}}$$
    $$S_{k|k-1} = HP_{k|k-1}H^T + R$$
    $$K_k = P_{k|k-1}H^T S_{k|k-1}^{-1}$$

3.3.3 Unscented Kalman Filter

The Unscented Transformation is a method to statistically linearize a non-linear function of a random variable. In this method, n points called sigma points are selected deterministically from prior distribution of a random variable and propagated through the non-linear function [36]. These propagated points form a statistics that can be used to estimate non-linearly transformed mean and variance [40]. The Unscented Kalman filter (UKF) uses unscented transformation in the implementation of Kalman filter [35]. Since EKF has limitations like difficult to calculate or non-existent $Jacobian$ matrices and non-accuracy of inaccurate error propagation, the UKF was proposed to overcome these deficiencies.

3.4 Sensor Fusion

In localization and tracking of an object, various types of sensors are used. Basically, these sensors are classified in two different groups which are relative (inertial) and absolute position sensors in [41]. The relative sensor gives information about its situation relative to its previous state. Gyroscope, accelerometer and magnetometer are examples of this type of sensors. The absolute positioning is based on information of node's location relative to a reference point at a known position and most popular example of it is GPS. Both sensor types have advantages and disadvantages that deeply affect the performance of the positioning and tracking. Generally inertial sensors have ability to give good results for short time intervals but they suffers from drift for extended periods of time. On the other hand, absolute position sensors may not provide the measurements all the time during the estimation due to communication problems and environmental obstacles.

Generally, both of these sensors are fused for enhancing performance of estimation by using their strengths. For example, the absolute measurements techniques like TOA, TDOA, AOA and RSSI can be combined with the relative sensors like accelerometer, gyroscope, magnetometer and compass. For the fusion process, Kalman filter and its variants are commonly used, GPS/IMU fusion for positioning with Kalman filter is provided in [11]. In [14], pedestrian localization in indoor environments by TDOA/IMU fusion is given where the IMU is used for step detection and orientation estimation by EKF.

Our objective is enhancing the performance of RSS based tracking by implementing RSS/IMU fusion. In [12], RSS measurements and velocity measurements from IMU are fused and it is shown that sensor fusion technique reduces the drift caused by IMU. In addition the approach is powerful against fluctuations on the RSSI measurements. Achieved results are 1 meter root mean square error on each axis. In [13], another fusion technique is proposed which combines RSS and IMU measurements taken by a smartphone. Firstly, orientation, position and velocity states are estimated with Sequential Monte Carlo Kalman filter (SMC-KF), secondly position of the node is estimated with the proposed RSS based localization algorithm and lastly both of the measurements (IMU and RSSI) are combined by a navigation filter which consists of

SMC filter and Kalman filter. As a result, sensor fusuion reduces the position error around $\%35$ compared to only-RSS case.

3.4.1 IMU Measurement Model

In general, IMUs consist of three dimensional (3D) gyroscopes, 3D accelerometers and 3D magnetometers based on Micro-Electro-Mechanical Systems (MEMS). The local magnetic field is obtained by the magnetometers. Nearly all modern gyroscopes measure angular velocity or rate-of-turn whereas conventional gyroscopes measure orientation. The accelerometers sense both linear acceleration and gravity. In [42], the accelerometer measurements are modeled with external specific force which consists of linear acceleration and Earth's gravitational field g, bias and Gaussian noise as follows

$$y_a = f + b_a + e_a \tag{3.16}$$

where y_a is the measurement, f is the external specific force, b_a is a slowly time-varying bias and e_a is the i.i.d. Gaussian noise. In our simulations, perfect orientation is assumed. Gravitational force part is subtracted so that the external specific force is equal to linear acceleration on each axis. In addition, the bias is not included in our model. Simplified model for our problem is as follows

$$y_a = l_a + e_a \tag{3.17}$$

where l_a is the linear acceleration.

3.5 Simulation Results

For the simulations, we generated a trajectory in a room to be followed by a blind-folded node and we deployed 4 anchors at the corners of the room given in Figure 3.1. The tracking algorithms are implemented for two cases to analyze how the sensor fusion affects estimation of the true trajectory. In the first case only RSS measurements

are available whereas RSS and acceleration (IMU) measurements are fused in the second case. Static localization is implemented for only RSS measurements. Kalman filter, Serial and Parallel EKF algorithms are implemented for both only RSS and RSS/IMU sensor fusion cases.

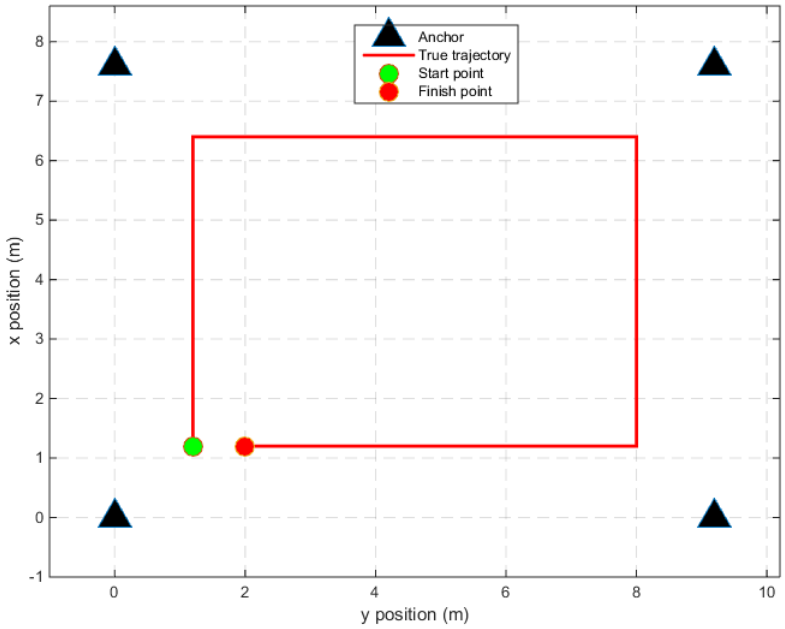

Figure 3.1: True trajectory of blindfolded node

For the Kalman filter, firstly static locations of blindfolded node are estimated from RSS measurements by MLE method given in Section 2.3.1, then these position estimates are used as measurements in the Kalman filter. For the serial and parallel EKF, RSS values are used as measurements directly in the filters.

In RSS/IMU fusion case, acceleration measurements on both x and y axes are taken with the frequency of 20 Hz. RSS measurements are taken with the frequency of 2 Hz, i.e., 2 RSS measurements are taken each second. When RSS measurement is available measurement update part of the filter is made with the RSS measurements. The sensor fusion algorithm is given in Table 3.5

In order to compare the filters in position RMSE sense, 500 MC runs are made to calculate the RMSE values of the filters. Initial values and simulation parameters are given in Table 3.6. The standard deviation of the acceleration is calculated by taking

TABLE 3.5: *Sensor Fusion*

- Initialization with $\hat{x}_{0|0}$, $P_{0|0}$ and $k = 1$
- For each k

  1-Prediction Update

  calculate $\hat{x}_{k|k-1}$ and $P_{k|k-1}$

  2 Measurement Updates

  calculate $\hat{x}_{k|k}$ and $P_{k|k}$ with acceleration data

  if (RSS measurement is available)

  {

  firstly, take the estimated state and covariance

  as predicted state and covariance as follows

  $\hat{x}_{k|k-1} = \hat{x}_{k|k}$

  $P_{k|k-1} = P_{k|k}$

  then, calculate $\hat{x}_{k|k}$ and $P_{k|k}$ with RSS measurements

  }

several measurements from the smartphone's (Iphone 5) accelerometer.

TABLE 3.6: *Simulation Parameters*

Simulation Parameters	
Path loss exponent α	3
Standard deviation of RSS σ_{RSS}	6 dB
First meter power of RSS P_0	-48 dBm
Standard deviation of acceleration σ_{ACC}	0.0152 m/s^2

In filters we use constant acceleration model given in (3.11) and the measurement model given in (2.2). Acceleration measurement model is linear and $h(x_k)$ for the acceleration measurements is given as

$$h(x_k) = H_{acc} = \begin{bmatrix} 0 & 0 & 1 & 0 & 0 & 0 \\ 0 & 0 & 0 & 0 & 0 & 1 \end{bmatrix}. \tag{3.18}$$

Initial state $\hat{x}_{0|0}$ which is obtained from static localization (MLE) by using RSS measurements and initial covariance $P_{0|0}$ matrices, where (1,1) and (4,4) elements are obtained from averaging Mean Squared Error (MSE) of static localization over 500 Monte Carlo runs for both x and y axes, are given as follows

$$\hat{x}_{0|0} = \begin{bmatrix} \hat{x}_{MLE(RSS)} & 0 & 0 & \hat{y}_{MLE(RSS)} & 0 & 0 \end{bmatrix}^T \tag{3.19}$$

$$P_{0|0} = \begin{bmatrix} MSE_{(MLE)}(\hat{x}) & 0 & 0 & 0 & 0 & 0 \\ 0 & 0.0065 & 0 & 0 & 0 & 0 \\ 0 & 0 & 0.00023 & 0 & 0 & 0 \\ 0 & 0 & 0 & MSE_{(MLE)}(\hat{y}) & 0 & 0 \\ 0 & 0 & 0 & 0 & 0.0065 & 0 \\ 0 & 0 & 0 & 0 & 0 & 0.00023 \end{bmatrix} \tag{3.20}$$

Measurement noise covariance for KF is formed from the MSE values of static localization (MLE) as follows

$$R = \begin{bmatrix} MSE_{(MLE)}(\hat{x}) & 0 \\ 0 & MSE_{(MLE)}(\hat{y}) \end{bmatrix}. \tag{3.21}$$

The measurement covariances of the other filters are taken as

$$R_{RSS} = \sigma^2_{RSS} \times I_4 \tag{3.22}$$

$$R_{ACC} = \sigma^2_{ACC} \times I_2 \tag{3.23}$$

with the identity matrix I. Lastly, the process noise covariance matrix is set as follows

$$Q = 0.000023 \times I_6. \tag{3.24}$$

- Figure 3.2 gives the drift of the position estimate from Kalman Filter by using only the acceleration data. As it seen in the figure, the position error increases over the time and reaches to 24 meter after 80 seconds because the error of the acceleration accumulates while estimating the position.
- Figure 3.3 indicates the comparison of performance of the static localization and tracking filters in the sense of RMSE for ONLY RSS case. When the blindfolded node approaches to the anchors, error of the MLE decreases. As it is seen, filters outperforms the localization (MLE) and using the positions estimated by MLE as a measurement in the Kalman filter gives better results. At the turning points, the filter performances decrease since we used constant acceleration model in our implementations and sharp turnings do not match the model.
- Figure 3.4 shows the RMSE performance of the filters for RSS/IMU fusion case and errors are near 1.5 meter. Figures 3.5-3.7 shows the comparison of the ONLY RSS and RSS/IMU fusion cases for each filter. Sensor fusion decreases the error approximately $\%$ 30 for the given measurement variances. All filter results for both cases are given in Figure 3.8.
- Figure 3.9 shows the CDF of tracking algorithms for ONLY RSS case. It is seen that there are errors up to 5 m for the serial and parallel EKF. In Figure 3.10, CDF of tracking algorithm for RSS/IMU fusion cases is presented and in this scenario 4 m errors are seen for serial and parallel EKF. Comparison of all CDFs is presented in Figure 3.11.

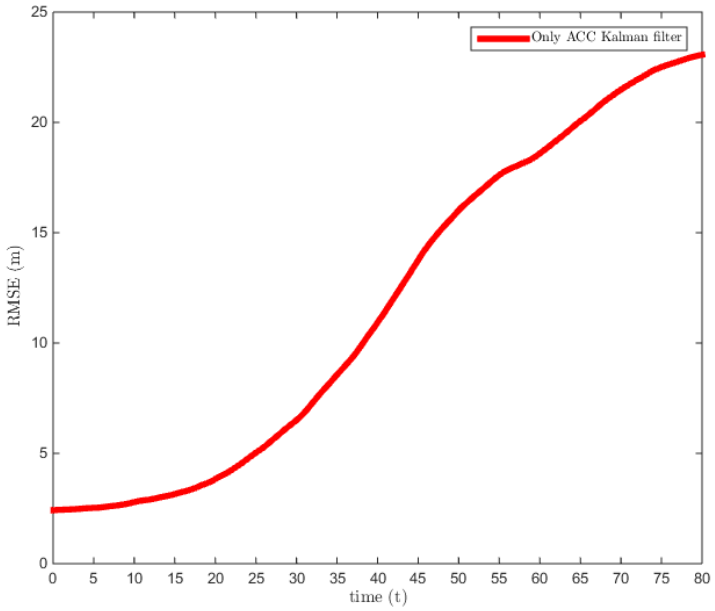

Figure 3.2: Tracking with ONLY ACC measurements

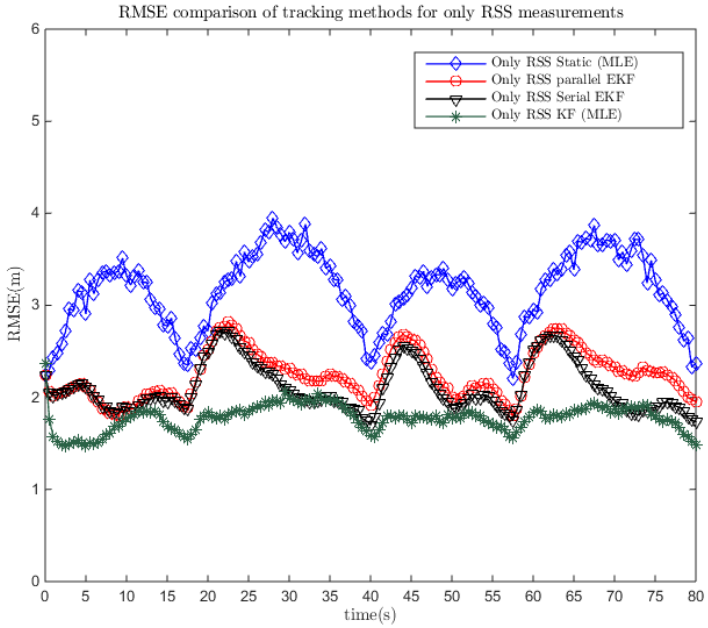

Figure 3.3: RMSE comparison of tracking algorithms with ONLY RSS measurements

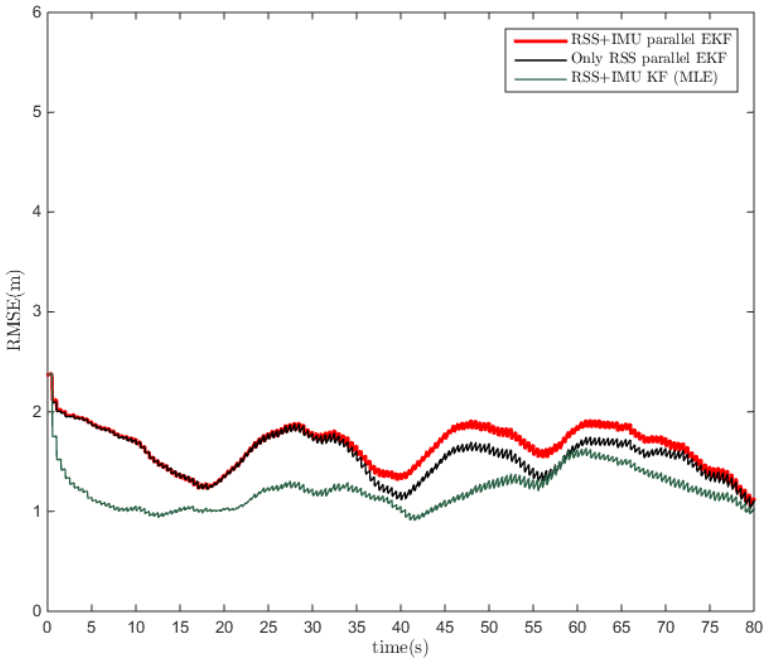

Figure 3.4: RMSE comparison of tracking algorithms for RSS/IMU fusion case

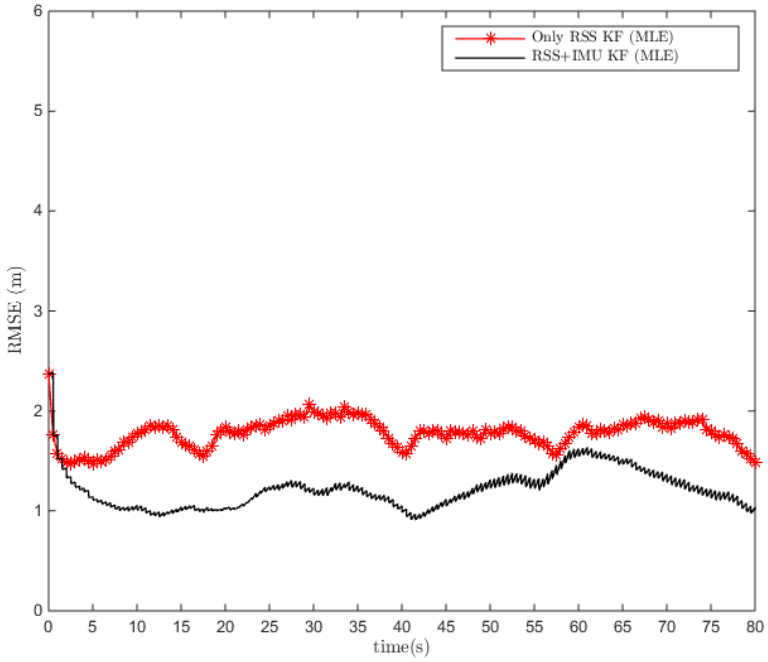

Figure 3.5: RMSE comparison of Kalman filter for ONLY RSS and RSS/IMU fusion cases

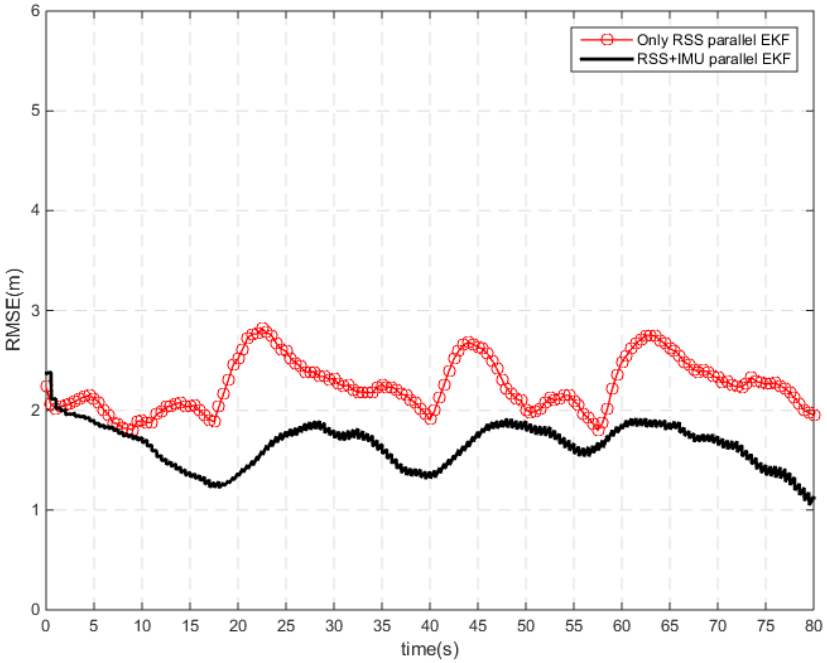

Figure 3.6: RMSE comparison of Parallel EKF for ONLY RSS and RSS/IMU fusion cases

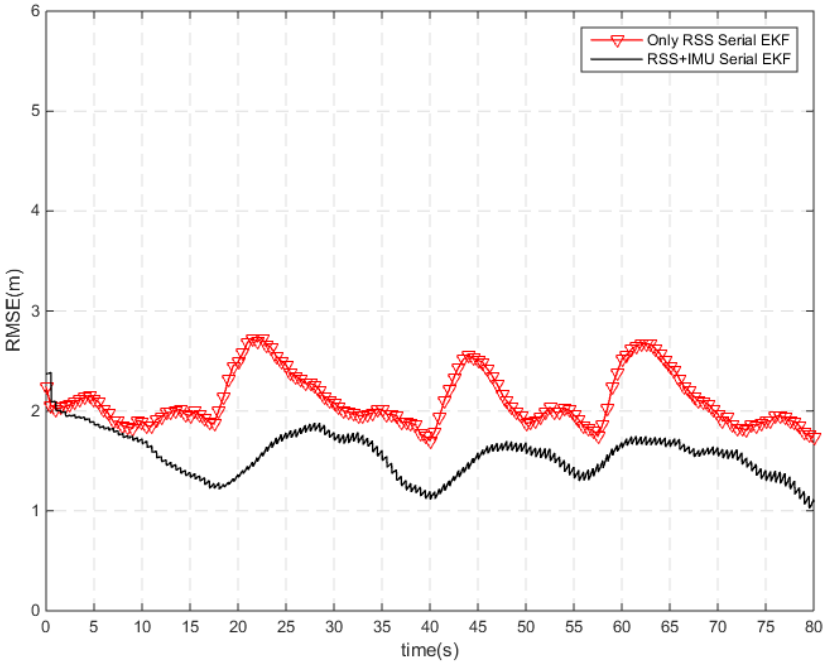

Figure 3.7: RMSE comparison of Serial EKF for ONLY RSS and RSS/IMU fusion cases

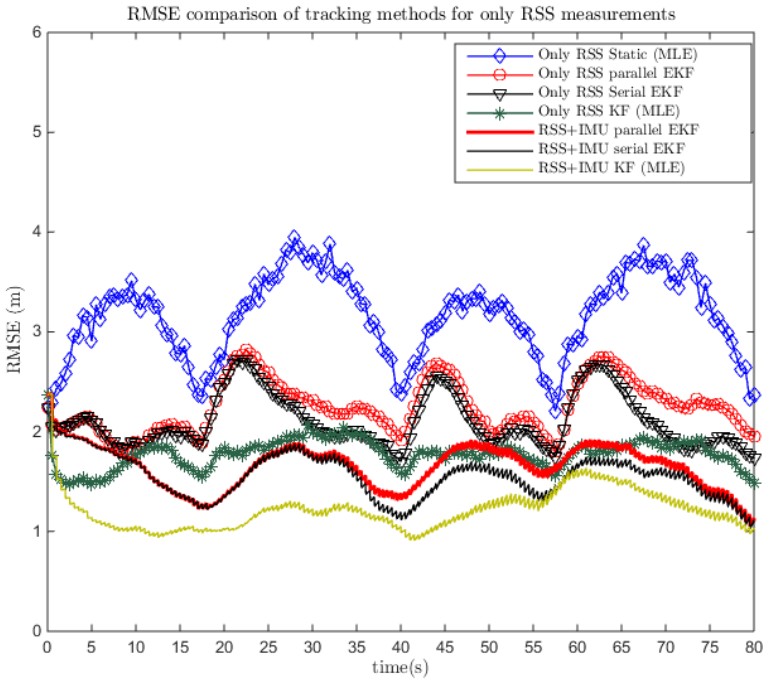

Figure 3.8: RMSE comparison of all filters for ONLY RSS and RSS/IMU fusion cases

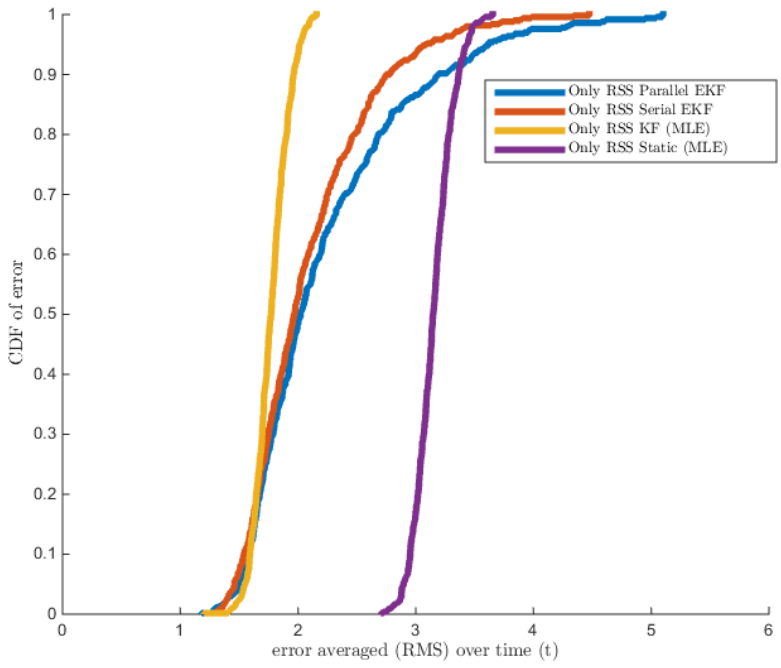

Figure 3.9: CDF of tracking algorithms for ONLY RSS

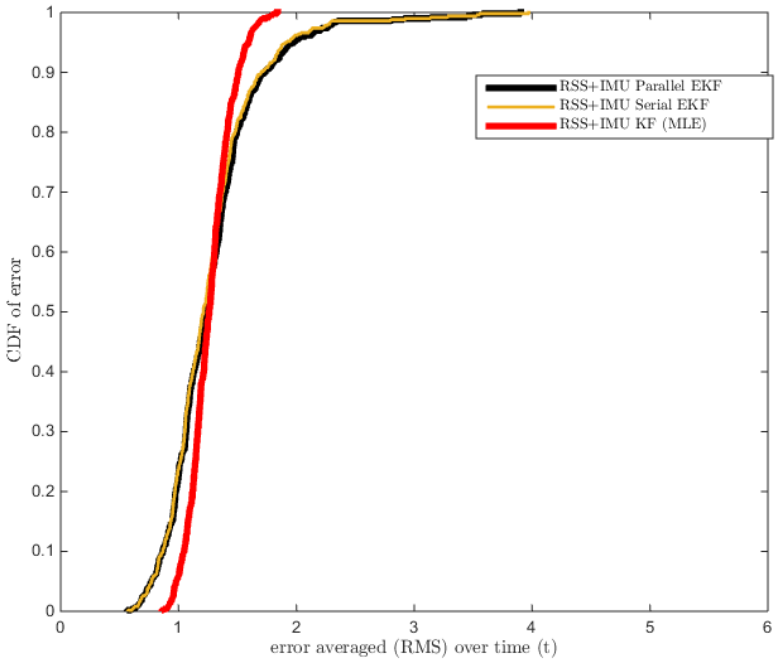

Figure 3.10: CDF of tracking algorithms for RSS/IMU fusion case

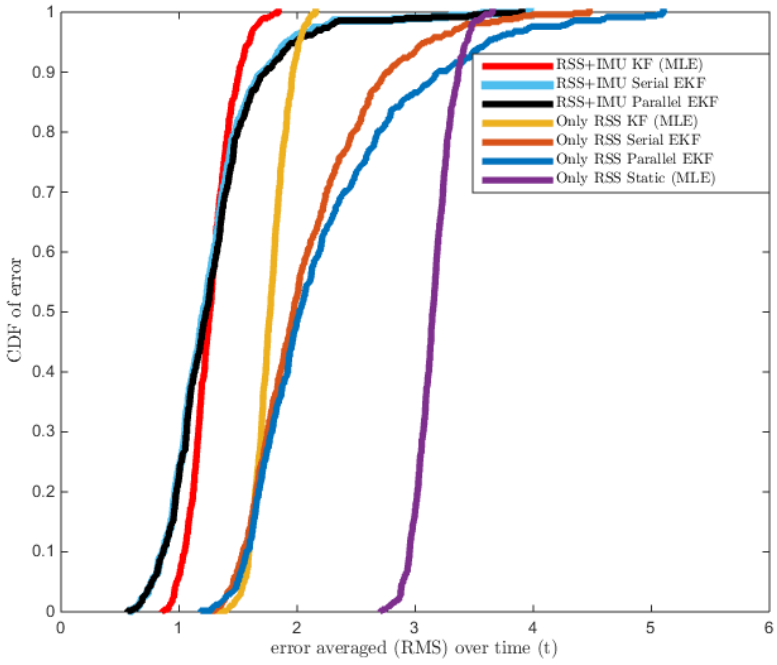

Figure 3.11: CDF of tracking algorithms for ONLY RSS and RSS/IMU fusion cases

3.5.1 Effects of the Measurement Variances

The reliability of the measurements is crucial for the localization and tracking performance. In the wireless system, a channel depends on time, frequency and space that affects the measurements. Because of these dependencies on the wireless channel, various factors affect the RSSI and cause variation. We can divide these factors into groups such as hardware based, environmental based, human based, spatial and interference. These factors are examined experimentally in [43]. It is possible to use time, frequency and space dimensions to our advantage with various techniques in order to acquire more reliable RSS samples. For example, changing the operating frequency among the multiple carrier frequencies (frequency hopping) is a widely used technique since different channels may have dissimilar characteristics. Time diversity and space/orientation diversity are also used for enhancing the RSS based localization performance. The variation of the RSS can be decreased with the use of such techniques.

The Inertial Measurement Unit (IMU) is another measurement source used in localization and tracking systems. Inertial sensors are generally classified according to their performance. In the market, one can encounter navigational (high precision), tactical, industrial and consumer grade (low precision) IMUs. The navigational (marine) IMUs serve the best position and orientation estimate yet their cost can reach over 1 million dollars. The cheapest one is consumer grade with the poorest performance. In this case the errors in the position estimates from the accelerometer data is enormous even if bias is little on the acceleration. A user's acceleration is obtained when the gravitational source is subtracted out from measurements, but orientation estimation is needed and the error from this estimation can cause a bias on the acceleration. Hence it is really difficult to obtain sufficient data from low cost IMU.

In this part, filter performances are analyzed depending on both RSS and acceleration standard deviations. The results are presented in Table 3.7-3.12.

- In Table 3.7, results of 500 MC runs for the ONLY RSS case are documented for different RSS standard deviations. Localization error is around 1.75 m where the filters can reach 1 m error while the standard deviation of the RSS is 3 dB.

- In Table 3.8, sensor fusion is analyzed with respect to RSS standard deviation while keeping the acceleration standard deviation fixed at $0.015m/s^2$. As seen in the table, tracking errors can be reduced to around 0.7 meter while the σRSS is 3 dB.
- Table 3.9 shows the sensor fusion performance with respect to acceleration data precision while keeping the σRSS fixed at 6 dB. The error is nearly 1 meter when the σACC is reduced to half.
- As we see in the Table 3.10, 0.54 meter error performance is attainable with the sensor fusion where the RSS std. dev. is $3\ dB$ and the acceleration std. dev. is $0.0015\ m/s^2$.

TABLE 3.7: *RMSE (m) values of ONLY RSS cases for different σRSS values*

σRSS	**STATIC (MLE)**	**PARALLEL EKF**	**SERIAL EKF**	**KALMAN FILTER**
6	3.13490	2.18142	2.05910	1.76425
5	2.69558	1.87645	1.77750	1.55707
4	2.24157	1.44799	1,40324	1.30112
3	1.76306	1.02954	1.02867	1.06386

TABLE 3.8: *RMSE (m) values of RSS/IMU fusion cases for different σRSS values (σACC = 0.015 m/s^2)*

σRSS	**PARALLEL EKF**	**SERIAL EKF**	**KALMAN FILTER**
6	1.53588	1.47114	1.33647
5	1.36404	1.38344	1.21088
4	1.10589	1.07392	0.99653
3	0.73603	0.72799	0.75795

TABLE 3.9: *RMSE (m) values of RSS/IMU fusion cases for different σACC values (σRSS = 6 dB)*

σACC	**PARALLEL EKF**	**SERIAL EKF**	**KALMAN FILTER**
0.015	1.53588	1.47114	1.33647
0.0075	0.97440	0.96381	1.02247
0.0015	0.93956	0,89362	0.98124
0.00075	0.86364	0.86023	0.95592

TABLE 3.10: *RMSE (m) values of RSS/IMU fusion cases for different σACC values (σRSS = 3 dB)*

σACC	**PARALLEL EKF**	**SERIAL EKF**	**KALMAN FILTER**
0.0075	0.56841	0.56763	0.70763
0.0015	0.54128	0.54681	0.63786

3.5.2 Effects of the Path Loss Exponent

In RSS-based localization, the path loss exponent is a significant factor which depends on the local environment and differs from channel to channel. Typical path loss exponents are given in [17] for different environments. In the buildings, the PLE's range is 1.6 to 3.5 when the receiver and transmitter at the same floor, for multiple floors the PLE is between 2 and 6. However, attenuations due to obstacles in buildings expands the range of empirical PLE. In Table 3.11 performances of localization and tracking algorithms for ONLY RSS case versus path loss exponent are given. As it seen in the table, errors tend to be higher at the low PLEs. The results for RSS+IMU fusion case according to PLE are shown in Table 3.12. As a conclusion, all performances for both cases are inversely proportional to the PLE.

TABLE 3.11: *RMSE (m) values of ONLY RSS cases for different α (path loss exponent) values (σRSS = 6 dB, σACC = 0.015 m/s^2)*

α	**STATIC (MLE)**	**PARALLEL EKF**	**SERIAL EKF**	**KALMAN FILTER**
4	2.47592	1.66968	1.55112	1.41389
3.5	2.74735	1.90181	1.79137	1.54108
3	3.14158	2.16087	2.07628	1.78011
2.50	3.63913	2.73508	2.48623	2.22456
2	4.45352	3.32225	3.09149	2.77758
1.50	5.61991	4.46848	4.13585	3.46903

TABLE 3.12: *RMSE (m) values of RSS/IMU fusion cases for different α (path loss exponent) values (σRSS = 6, σACC = 0.015 m/s^2)*

α	**PARALLEL EKF**	**SERIAL EKF**	**KALMAN FILTER**
4	0.94086	0.94825	1.07331
3.5	1.15682	1.14536	1.11483
3	1.49482	1.48357	1.37007
2.50	1.66790	1.62269	1.52969
2	2.00511	1.88616	1.69568
1.50	2.37407	2.32365	1.93667

CHAPTER 4

POSTERIOR CRAMER RAO BOUND FOR FILTERING

One common bound on the performance of an estimator is conventional Cramér-Rao lower bound (CRLB) [44]. The CRLB gives a minimum achievable variance for any unbiased estimator of a non-random parameter. This bound provides opportunity to compare the implemented algorithms and had been used as a benchmark to compare estimators with each other. So, CRLB gives information about the reachable maximum performance of a system before implementing it and can be considered as a system design tool.

Since CRLB is a bound for static estimation problems, it is not convenient for tracking problems because the states are changing dynamically. For random parameters, a lower bound that is analogous to CRLB is presented by Van Trees in [44]. This bound is called as posterior CRLB (PCRLB) or Bayesian CRLB and given by the inverse of Fisher Information Matrix (FIM) for a random vector.

In the derivation of FIM for the PCRLB, the expectations are taken with respect to the joint distribution of the states and the measurements which is $p(x_k, y_k)$ for the time k. Since these expectations takes averages over the measurements, the PCRLB is an off-line bound and is derived from only the initial state, the measurement model and the state space model.

Considering a vector of states $X_k = [x_0, x_1, ..., x_k]$ and its estimate $\hat{X}_{k|k}$ based on the measurements $Y_k = [y_1, y_2, ..., y_k]$, the CRLB for vector parameters can be written as

the inverse of the FIM J_k [29]

$$MSE(\hat{X}_{k|k}) = \mathbb{E}\big\{(\hat{X}_{k|k} - X_k)(\hat{X}_{k|k} - X_k)^T\big\} \geq {J_k}^{-1} \tag{4.1}$$

$$J_k = \mathbb{E}\big\{[\bigtriangledown_{X_k} \log p(X_k, Y_k)][\bigtriangledown_{X_k} \log p(X_k, Y_k)]^T\big\} \tag{4.2}$$

where $\bigtriangledown_{X_k}$ is a first-order partial derivative with respect to X_k.

4.1 Posterior Cramer Rao Lower Bound For Filtering

Since the CRLB depends on the assumption of the deterministic state variables, Van Trees proposed a new bound for the non-deterministic parameters which is posterior CRLB in [44]. Consider the general form for the state and measurement models

$$x_k = f(x_{k-1}) + w_k \tag{4.3}$$

$$y_k = h(x_k) + v_k \tag{4.4}$$

the PCRLB which bounds the estimate covariance is given as follows

$$MSE(\hat{X}_{k|k}) = \mathbb{E}\big\{(\hat{X}_{k|k} - X_k)(\hat{X}_{k|k} - X_k)^T\big\} \geq {J_k}^{-1} \tag{4.5}$$

$$J_k = \mathbb{E}\big\{ - \bigtriangledown_{X_k} \bigtriangledown_{X_k}^T \log p(X_k, Y_k)\big\} \tag{4.6}$$

where the partial derivatives in equation (4.6) are calculated at the true state and the expectation is taken with respect to Y_k and X_k different from the CRLB where the expectation is taken over the only Y_k. As the time k increases, the PCRLB becomes difficult to compute due to the large data processing. Thankfully, in [45] Tichavsky *et al.* proposed a recursive solution for calculation of the PCRLB.

Suppose that X_k is a sequence of the n-dimensional states and the corresponding FIM is J with the dimension $(nk \times nk)$. J_k is the $(n \times n)$ dimensional FIM for the state x_k and the sequence $(J_1, J_2, ..., J_k)$ is the FIM matrices for the estimation of the states $(x_1, x_2, ..., x_k)$. Tichavsky derived the following recursive algorithm in order to obtain J_k.

$$J_{k+1} = D_k^{22} - D_k^{21}(J_k + D_k^{11})^{-1} D_k^{12} \tag{4.7}$$

where

$$D_k^{11} = \mathbb{E}_{p(x_{k+1},x_k)}\big\{ - \bigtriangledown_{x_k} \bigtriangledown_{x_k}^T \log p(x_{k+1}|x_k)\big\} \tag{4.8}$$

$$D_k^{12} = (D_k^{21})^T = \mathbb{E}_{p(x_{k+1},x_k)}\big\{ - \bigtriangledown_{x_k} \bigtriangledown_{x_{k+1}}^T \log p(x_{k+1}|x_k)\big\} \tag{4.9}$$

$$\begin{aligned} D_k^{22} &= \mathbb{E}_{p(x_{k+1},x_k)}\big\{ - \bigtriangledown_{x_{k+1}} \bigtriangledown_{x_{k+1}}^T \log p(x_{k+1}|x_k)\big\} \\ &\quad + \mathbb{E}_{p(x_{k+1},y_{k+1})}\big\{ - \bigtriangledown_{x_{k+1}} \bigtriangledown_{x_{k+1}}^T \log p(y_{k+1}|x_{k+1})\big\} \\ &= D_k^{22,a} + D_k^{22,b} \end{aligned} \tag{4.10}$$

with the initial value

$$J_0 = \mathbb{E}\big\{ - \bigtriangledown_{x_0} \bigtriangledown_{x_0}^T \log p(x_0)\big\}. \tag{4.11}$$

For the case of the linear and Gaussian system given in equation (3.12), conditional pdfs of $p(x_{k+1}|x_k)$ and $p(y_k|x_k)$ are given as follows.

$$p(x_{k+1}|x_k) = \frac{1}{(2\pi)^2|Q_k|^{1/2}} \exp[-(1/2)(x_{k+1} - A_k x_k)^T Q_k^{-1}(x_{k+1} - A_k x_k)] \tag{4.12}$$

$$p(y_k|x_k) = \frac{1}{(2\pi)^2|R_k|^{1/2}} \exp[-(1/2)(y_k - H_k x_k)^T R_k^{-1}(y_k - H_k x_k)] \tag{4.13}$$

where $|Q_k|$ and $|R_k|$ are the determinants of Q_k and R_k respectively. It can easily be shown that

$$D_k^{11} = A_k^T Q_k^{-1} A_k \tag{4.14}$$

$$D_k^{12} = (D_k^{21})^T = -A_k^T Q_k^{-1} \tag{4.15}$$

$$D_k^{22} = Q_k^{-1} + H_{k+1}^T R_{k+1}^{-1} H_{k+1} \tag{4.16}$$

However, for the non-linear measurement model such as RSS measurement model given in equation (2.2), the expectation in $D_k^{22,b}$ involves a highly nonlinear function and is not analytically tractable. In order to calculate this expectation, Monte Carlo random sampling methods are usually used.

4.1.1 Monte Carlo Approximation for the PCRLB

For the non-linear measurement model, $D_k^{22,b}$ term of the recursive PCRLB equation requires the knowledge of $p(x_{k+1}, y_{k+1})$. Based on the assumption of the zero mean Gaussian measurement noise we have

$$\begin{aligned} \bigtriangledown_{x_{k+1}} \log p(y_{k+1}|x_{k+1}) &= \bigtriangledown_{x_{k+1}} \Big[-\frac{1}{2}[y_{k+1} - h(x_{k+1})]^T R_{k+1}^{-1}[y_{k+1} - h(x_{k+1})] \Big] \\ &= \big[\bigtriangledown_{x_{k+1}} h(x_{k+1})^T \big] R_{k+1}^{-1} \big[y_{k+1} - h(x_{k+1}) \big] \end{aligned} \tag{4.17}$$

and $D_k^{22,b}$ matrix given in (4.10) can be further computed as

$$\begin{aligned} D_k^{22,b} &= \mathbb{E}_{p(x_{k+1},y_{k+1})} \Big\{ \big[\bigtriangledown_{x_{k+1}} \log p(y_{k+1}|x_{k+1}) \big] \big[\bigtriangledown_{x_{k+1}} \log p(y_{k+1}|x_{k+1}) \big]^T \Big\} \\ &= \mathbb{E}_{p(x_{k+1},y_{k+1})} \Big\{ \big[\bigtriangledown_{x_{k+1}} h(x_{k+1})^T \big] R_{k+1}^{-1} \big[\bigtriangledown_{x_{k+1}} h(x_{k+1})^T \big]^T \Big\} \\ &= \mathbb{E}_{p(x_{k+1},y_{k+1})} \Big\{ H_{k+1}^T R_{k+1}^{-1} H_{k+1} \Big\} \end{aligned} \tag{4.18}$$

where H_{k+1} is the Jacobian of $h(x_{k+1})$ evaluated at the true value of x_{k+1} and R_{k+1} is the corresponding measurement noise covariance.

Let

$$\wedge_k^{22,b}(x_{k+1}) \triangleq H_{k+1}^T R_{k+1}^{-1} H_{k+1} \tag{4.19}$$

then the equation (4.18) can be represented as simply form

$$
\begin{aligned}
D_k^{22,b} = \mathbb{E}\big\{ \wedge_k^{22,b}(x_{k+1})\big\} &= \int\int \wedge_k^{22,b}(x_{k+1}) p(x_{k+1}, y_{k+1}) d_{x_{k+1}} d_{y_{k+1}} \\
&= \int \wedge_k^{22,b}(x_{k+1}) \Big(\int p(x_{k+1}, y_{k+1}) d_{y_{k+1}} \Big) d_{x_{k+1}} \\
&= \int \wedge_k^{22,b}(x_{k+1}) p(x_{k+1}) d_{x_{k+1}}.
\end{aligned} \tag{4.20}
$$

The expectation is taken with respect to the x_k only, since the bound is independent of the measurement sequence. In order to solve the expectation we can use Monte Carlo integration. So we need samples (namely particles) from the density $p(x_{k+1})$ for the MC integration. In the case of target tracking, we generate N trajectories $X_k^i = [x_0^i, x_1^i, ..., x_k^i]$, $i = 1, 2, ..N$ according to the state space model.

With the assumption of the state of ith trajectory at the time $k+1$ is a dirac delta function located in $\hat{x}_{k+1}^i$, then the empirical estimate of $p(x_{k+1})$ is given as follows

$$
\hat{p}_(x_{k+1}) = \frac{1}{N} \sum_{i=1}^{N} \delta(x_{k+1} - \hat{x}_{k+1}^i). \tag{4.21}
$$

Substituting this estimated density into (4.20) and by using the sifting Property of the delta function we have

$$
\begin{aligned}
D_k^{22,b} = \mathbb{E}\big\{ \wedge_k^{22,b}(x_{k+1})\big\} &= \int \wedge_k^{22,b}(x_{k+1}) p(x_{k+1}) d_{x_{k+1}} \\
&= \frac{1}{N} \sum_{i=1}^{N} \wedge_k^{22,b}(x_{k+1}) \delta(x_{k+1} - \hat{x}_{k+1}^i) \\
&= \frac{1}{N} \sum_{i=1}^{N} \wedge_k^{22,b}(\hat{x}_{k+1}^i).
\end{aligned} \tag{4.22}
$$

Now we are able to calculate the approximate posterior CRLB by Monte Carlo integration method.

4.1.2 Simulation Results

For the state vector given in (3.10), the position PCRLB at the time k given as

$$PCRLB = \sqrt{J_k^{-1}(1,1) + J_k^{-1}(4,4)} \tag{4.23}$$

where $J_k^{-1}(1,1)$ and $J_k^{-1}(4,4)$ are the elements of the J_k^{-1} related to positions at x and y axis respectively. The initial information matrix J_0 depends on the $p(x_o)$ as given in (4.11) and for the Gaussian case $J_0 = P_{0|0}^{-1}$ where $P_{0|0}$ is the initial covariance that was used in section 3.

For computing PCRLBs for the non-linear system, the same values of the measurement noise covariances of the RSS R_{RSS} and the acceleration R_{ACC}, the process noise covariance Q , initial values $\hat{x}_{0|0}$ and $P_{0|0}$ in Section 3 are used. Also, for the linear case the same measurement models and covariance matrix of the estimated locations by MLE in section 3 are used. We made 500 MC realizations for the same parameters in order to obtain simulation results .

For Kalman filter, system models (state and measurement) are both linear, hence the computation of the PCRLB is independent from the x_k. For the RSS/IMU fusion case, the equations for the recursive computation of the PCRLB for the linear and non-linear cases are given in Table 4.1.

TABLE 4.1: *Computation of the PCRLBs for the sensor fusion case*

Start from k=0, for each k

$D_k^{11} = A_k^T Q_k^{-1} A_k$

$D_k^{12} = (D_k^{21})^T = -A_k^T Q_k^{-1}$

- For the linear case

  if RSS measurement available at time k

  $D_k^{22} = Q_k^{-1} + H_{RSS-MLE,k+1}^T R_{RSS-MLE,k+1}^{-1} H_{RSS-MLE,k+1}$

  else

  $D_k^{22} = Q_k^{-1} + H_{ACC,k+1}^T R_{ACC,k+1}^{-1} H_{ACC,k+1}$

- For the non-linear case with the SMC approximation

  if RSS measurement available at time k

  $D_l^{22} = Q_k^{-1} + \mathbb{E}_{p(x_{k+1},y_{k+1})}\left\{ H_{RSS,k+1}^T R_{RSS,k+1}^{-1} H_{RSS,k+1} \right\}$

  else

  $D_k^{22} = Q_k^{-1} + H_{ACC,k+1}^T R_{ACC,k+1}^{-1} H_{ACC,k+1}$

where $H_{RSS,k+1}$ is the Jacobian of $h(x_{k+1})$, $H_{RSS-MLE,k+1}$ is the measurement matrix of the linear model for the estimated locations from the RSS measurements by MLE and $R_{RSS-MLE,k+1}$ is the measurement covariance matrix for the estimated locations from the RSS measurements by MLE.

Figures 4.1-4.4 shows the PCRLBs for the RSS based and RSS+IMU fusion based tracking systems where the blindfolded node follows the constant acceleration model exactly.

- In Figure 4.1, posterior CRLBs are given for the RSS standard deviations 6,5,4 and 3 dB respectively for non-linear measurement models. As seen, the bound goes under to 1 meter position error for 3 dB RSS standard deviation for ONLY RSS case. In sensor fusion, the bound is decreased to 0.5 meter for 3 dB σRSS.
- For linear measurement case, position estimates by MLE are considered as a measurement, PCRLBs with different RSS standard deviations are shown in Figure 4.2. The results are similar to non-linear case and the bound is near 1 meter while using only the RSS measurements with 3 dB standard deviation. Also sensor fusion is bounded with 0.5 meter for this value of standard devia-

tion.

- Precision of the acceleration data is also affecting the bounds for sensor fusion. Figure 4.3 PCRLBs for different σACC for non-linear measurement case. Average of the bounds are 0.96 m and 0.85 m for the standard deviations 0.15 m/s^2 and 0.005 m/s^2 respectively. Since the standard deviation of the process noise is 0.0048 in our system, change of the PCRLB is not remarkable when the standard deviation of the acceleration drops below the value 0.0048 m/s^2. Lower bounds are possible for the systems with low process noises. In Figure 4.4, the PCRLBs for the linear system are given according to different σACC values. Likewise the non-linear system, average of the bounds are 0.94 m and 0.83 m for the standard deviations 0.15 m/s^2 and 0.005 m/s^2 respectively.
- For Monte Carlo integration, 500 trajectories are generated that exactly follow the constant acceleration model given in 3.11. Each trajectory begins at any point which is selected arbitrarily in the area shown in Figure 3.1. A trajectory eventually leaves the area that is encircled by the anchor nodes after spending some time in that area. RSS measurements are dominant during the time spent in the encircled area. However when the blindfolded node leaves the encircled area, the acceleration measurements become dominant because of the increasing distances between blindfolded node and the anchors. As seen in the Figures 4.1-4.2, PCRLBs of the ONLY RSS cases deteriorate after some time. For our problem the deterioration occurs after spending approximately 3.5 seconds in the trajectory.

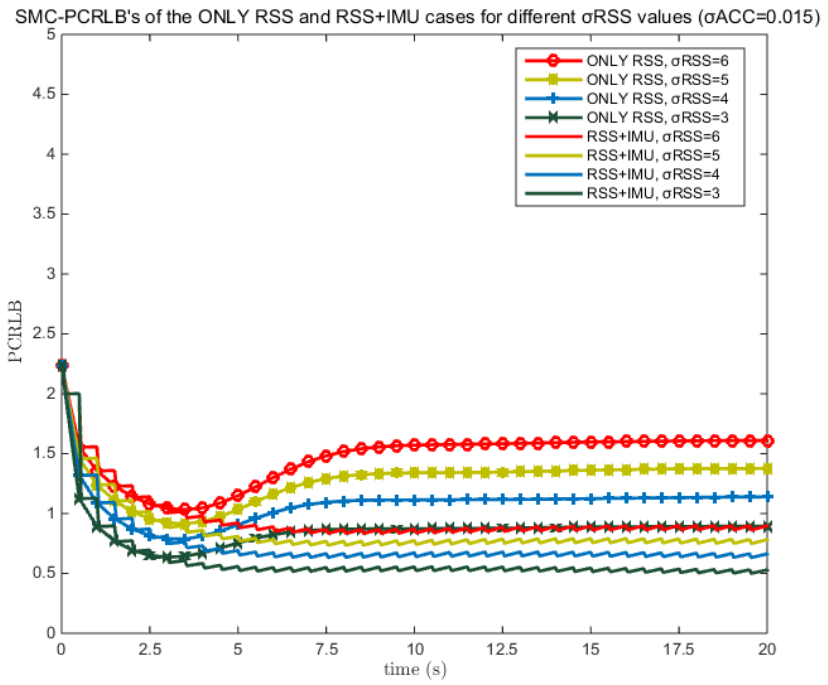

Figure 4.1: Position SMC-PCRLBs for different σRSS values

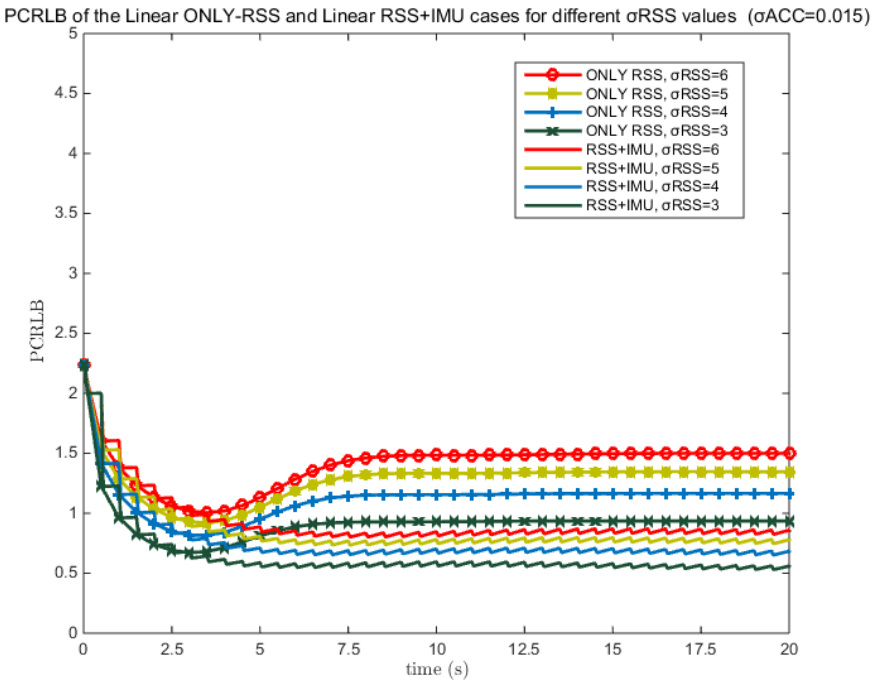

Figure 4.2: Position PCRLBs for different σRSS values

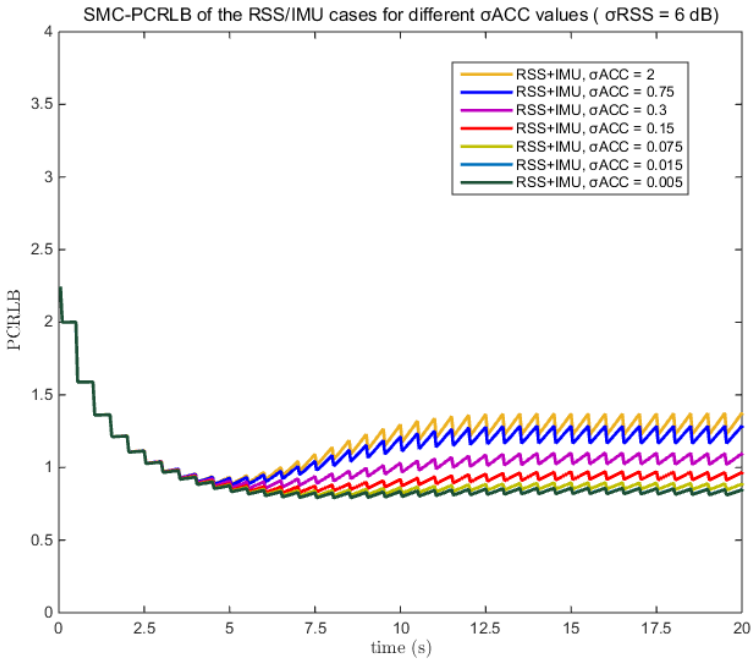

Figure 4.3: Position SMC-PCRLBs for RSS/IMU fusion case and for different σACC values

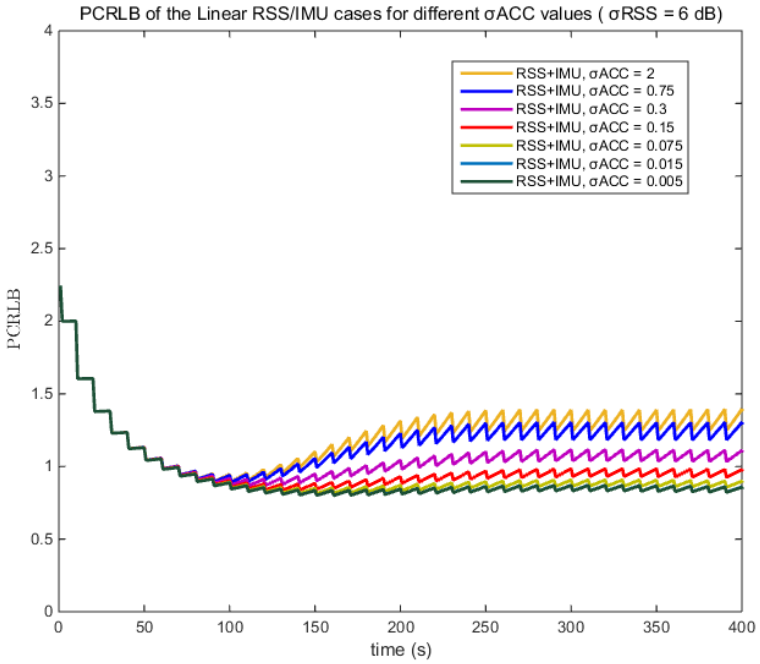

Figure 4.4: Position PCRLBs for Linear RSS/IMU fusion case and for different σACC values

CHAPTER 5

EXPERIMENTAL STUDY

5.1 Sensor Nodes

A sensor node in a WSN is usually required to be capable of sensing, processing the data and communicate with the other nodes in the network. In our study we used Arduino Uno R3 boards for the data processing, 2GB SD card for the memory applications and Xbee Series 2 RF modules which is mounted on the Arduino Wireless Shield to obtain a mesh network. Components of the sensor node are shown in Figure 5.1.

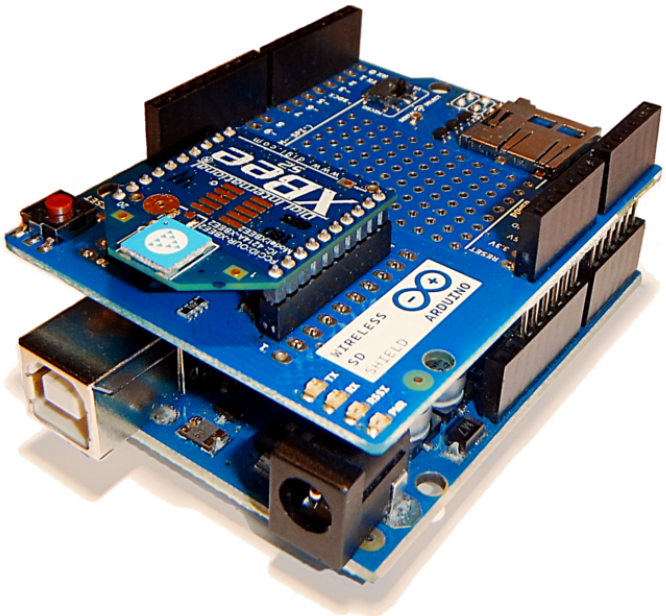

Figure 5.1: Complete Sensor Node

The Arduino Uno R3 boards are used as development boards based on the Atmega328 microcontroller, it is relatively easy to develop some applications consisting of electronics and coding on these boards. The specifications of the Arduino Uno R3 are enlisted in Table 5.1.

TABLE 5.1: *Arduino Uno R3 Specifications*

Microcontroller	ATmega328
Operating Voltage	5V
Input Voltage (recommended)	7-12V
Input Voltage (limits)	6-20V
Digital I/O Pins	14 (of which 6 provide PWM output)
Analog Input Pins	6
DC Current per I/OPin	40mA
DC Current per 3.3V pin	50mA
Flash Memory	32 KB
SRAM	2KB(ATmega328)
EEPROM	1KB(ATmega328)
Clock Speed	16 MHz

Since the usage of WSNs spreads to great variety of areas, different protocols are developed to build a network consisting of the sensor nodes. One of the most common protocols is Zigbee with low cost and low power consumption advantages. Xbee Series 2 RF modules which re used in this thesis use this protocol. Zigbee provides a short range wireless solution based on the mesh topology and it uses 2.4 GHz frequency band all over the world but there are some Xbee modules working in different frequencies like 868 Mhz and 900 Mhz as well.

Besides a communication between two modules, the Xbees enable star and mesh networks constellations. Each sensor node has a role in the network defined by Zigbee protocol and these roles are coordinator, router and end device. Each network can have only one coordinator which establishes the network and also stores the network information. The coordinator cannot be battery-powered. The routers are used as a relay in the network and can connect with the coordinator and the other devices.

The router also cannot be battery-powered since it must store the packets for the end devices. Lastly, end devices are usually used for the sensing and they are battery-powered. They can sleep for a certain time of period. A sample network topology is given in Figure 5.2. The transmit power of the Xbee is 2mW, i.e., 3 dBm, and the sensitivity of the receiver is -100 dBm.

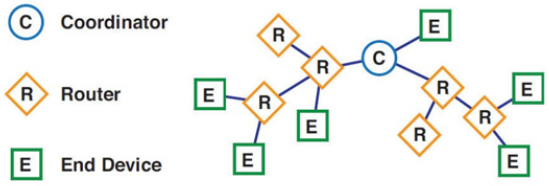

Figure 5.2: The Sample Zigbee Topology

Communication between the Arduino and the Xbee is established through a logic level asynchronous serial port. Both the Xbee and the Arduino have Universal Asynchronous Receiver/Transmitter Interface (UART) and with the same configuration of each UART, these devices communicate through a serial port. Pin connections of the Xbee and Arduino are shown in Figure 5.3. In our work, baud rate is 9600 bps, payload is 8 bits, before and after any byte 0 and 1 is sent respectively for synchronization.

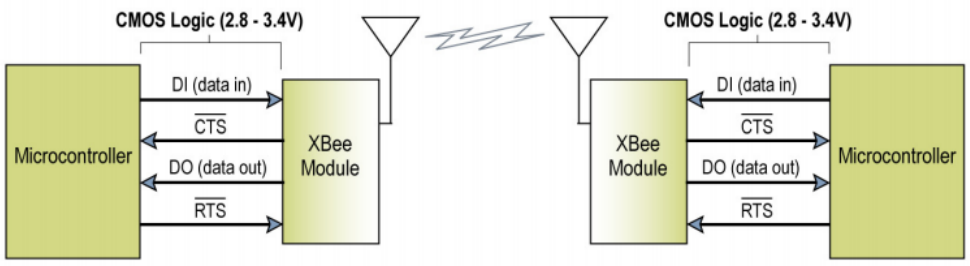

Figure 5.3: System Data Flow Diagram of Xbee and Microcontrollers

There are two serial communication modes of the Xbee, one of them is Transparent Mode (AT mode) and the other one is Application Programmable Interface (API) mode [46]. When operating in the AT mode, all information received from serial port of the Xbee is adjoined one after the other for wireless communication. In the case that the Xbee module cannot transmit instantly when it is busy with receiving a wire-

less packet, the UART data is saved in the buffer reserved for serial information. RF transmission of the serial data starts after Packetization Timeout (R0) is over or the maximum number of bytes in a packet (100 bytes) is received. In this mode, configuration of the Xbee (such as destination address, sleep time, I/O pins etc.) can be done by user via XCTU software or the host microcontroller by sending AT commands through the serial port. Digi's XCTU is a free software to interact with RF modules through a graphical interface which is easy to use.

Alternative to default Transparent Mode, the API mode enables arrangement of the network capabilities of the RF module from host application. API mode supports a frame based communication for all data entering or leaving the RF module. The host microcontroller sends a frame containing destination address, payload (data to be send) and all other transmission settings. On the receiver side, when the packet is received, receiver Xbee sends information frame by frame to the host control unit consist ofsender address, RSS of the last packet and actual content. Also Xbee series 2 modules save the RSS measurement of the last received packet and allow reaching this information with a DB command (AT) sent to the module. API mode enables to change destination address, communication channel and some other transmission options without entering the command mode.

In this work, we established a network containing 5 sensor nodes, one of them is coordinator (blindfolded), the others (anchors) are routers and all nodes operated in the API mode. The blindfolded node send a broadcast message and the anchors save the RSS value of the last received packet to the SD card which is mounted on the Arduino Wireless Shield SD extension. The destination address for the broadcast is 0xFFFF.

5.2 Estimation of the Channel Parameters

In order to estimate channel parameters which are path loss exponent α, first meter power P_0 and the standard deviation of RSS σ_{RSS}, we used Least Square (LS) estimation. LS aims to determine optimum values for variables that ensure the sum of the squared residuals between the observations and measurement predictions are

minimum. This is also known as fitting a line through the data. In [47], milimeter-wave propagation characteristics are discussed and PLE is estimated as the best fit minimum mean square error (MMSE) over a large amount of data.

We took the measurements in the communication laboratory of Gazi University which is located at Technology Faculty. The laboratory consists of the obstacles such as tables and computers. The measurements are taken at 24 fixed points shown in Figure 5.4. The blindfolded node sent 30 packets at each point and the all anchors saved the RSS values. Total number of the measurements used in parameter estimation is 3360.

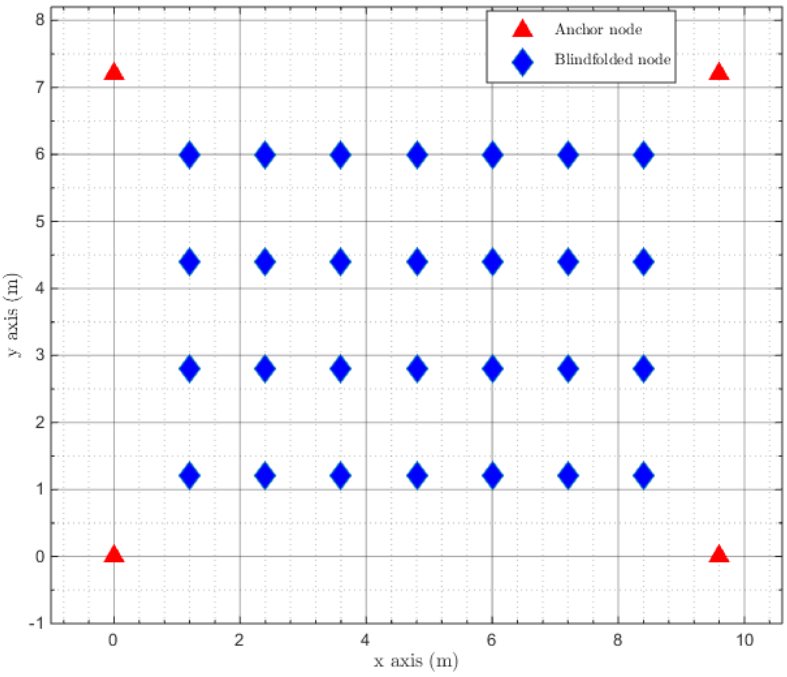

Figure 5.4: The Measurement Points for the Parameter Estimation

Considering the RSS measurement model given in equation 2.2, the Least Square estimation is made for the parameters PLE (α) and P_0 in a matrix form. The solution

is expressed as

$$\begin{bmatrix} \hat{P}_0 \\ \hat{\alpha} \end{bmatrix} = (H^T H)^{-1} H^T P \tag{5.1}$$

where $P = [P_1\ P_2\ ..\ P_m]^T$ is the measurement vector, $H = \left[\begin{array}{c:c} 1 & -10\log d \end{array}\right]$ where 1 is vector of ones and d is the vector of distances. The collected measurements and estimated path loss model is shown in Figure 5.4, the estimated path loss is given in Figure 5.5. P_0 estimate is -52 dBm, the path loss exponent estimate is α = 1.8 and σ_{RSS} estimate is 5.8 dB.

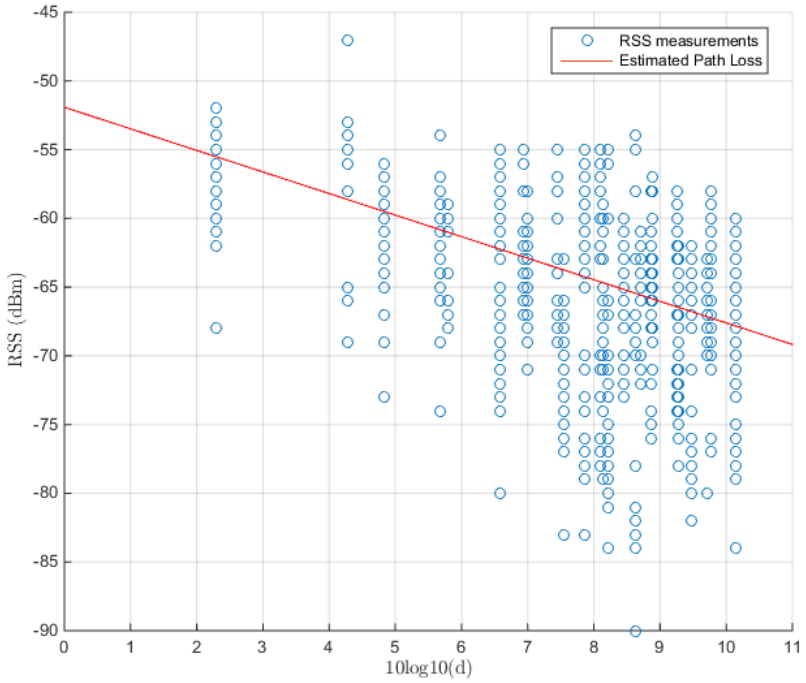

Figure 5.5: Estimated Path Loss

5.3 Antenna Performances of RSSI

RSSI based indoor localization and tracking systems use a great variety of antennas and antenna performance is crucial for the accuracy of the system. In the WSNs,

small antennas with non-isotropic gain patterns are usually used due to the necessity of the tiny and inexpensive devices. For the Xbee radio modules, chip antenna and wire antennas are available and in [48] different experiments are performed in order to analyze antenna performances. It is shown that anchor antennas should be at least 1 meter above from the ground for stable measurements. Also it is concluded that the antenna patterns are not isotropic and variance of the chip antenna is higher than the wire one. In [49], RSS based localization technique MLE, proximity based ECOLOCATION and finger printing algorithms' performances are compared experimentally for antenna orientations. Rather than a Xbee, CC2430 [50] radios work on 2.4 Ghz are used as a sensor node. Experiments are performed for the horizontal and vertical antenna orientations by taking measurements from various locations and using different frequencies. It is shown that antenna orientation has a great impact on RSS and RSS based localization

In our study, the antenna pattern analysis was done experimentally where anchor and the blindfolded node was placed one meter above the ground and the distance between the blindfolded node and the anchor was set to 2 m. The orientation of the anchor was fixed and 100 measurements were taken for each orientation of the blindfolded node. Later, these measurements were averaged. As shown in the Figure 5.6, radiation pattern of the chip antenna is not isotropic and variance of the RSS is substantial.

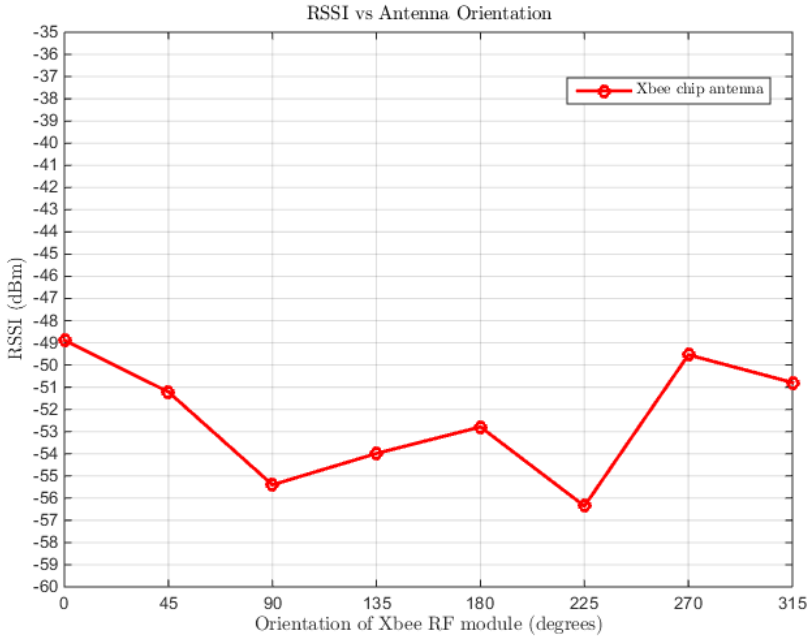

Figure 5.6: RSSI vs Antenna Orientation

5.4 Experimental Tracking

For the experimental study, we used a 7.6 m $\times$ 9.2 m area of the communication laboratory. We deployed the anchors at the corners of the area, anchor 1 at the point (0,0), anchor 2 at the point (7.6,0), anchor 3 at the point (7.6,9.2) and anchor 4 at the point (0,9.2). Our experimental trajectory was the same trajectory that was used in the simulation part. The blindfolded node followed the trajectory and sent a broadcast message with a packet number as a payload each 2 seconds. The anchors saved the RSS values of the each packet on the 2GB SD card. The RSS values obtained are shown in Figure 5.7. For the implementation of the algorithms, estimated channel parameters were used and the process noise was also the same as the one used in the simulation section. Experimental results of the tracking algorithms for both ONLY RSS and RSS+IMU cases are illustrated in the Figures 5.8-5.11.

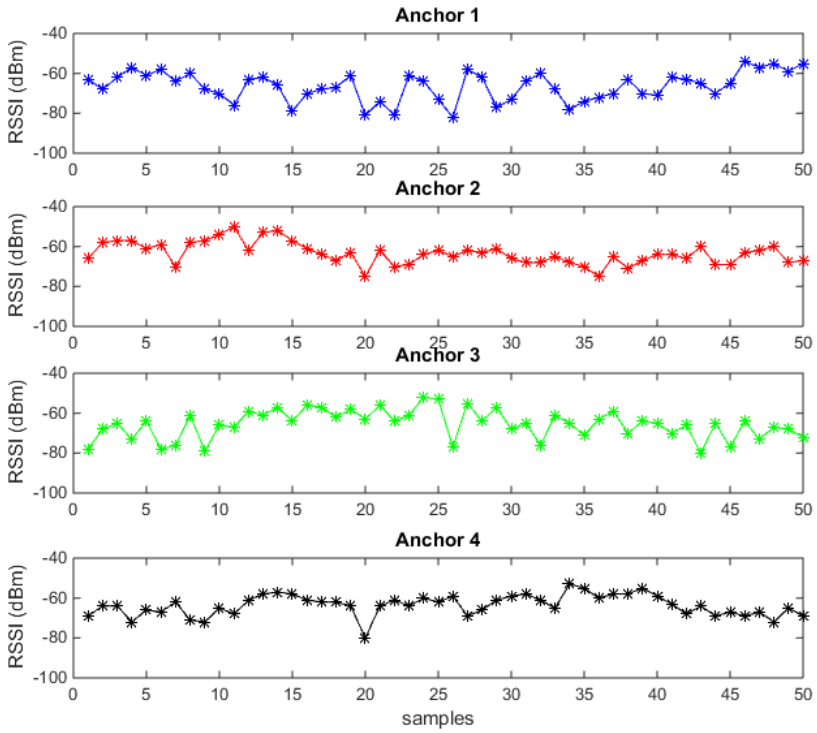

Figure 5.7: Experimental RSS measurements

- Estimated positions obtained by MLE algorithm with experimental data are given in Figure 5.8. The RMSE of the static localization is 3.16 m.
- In Figure 5.9, the performance of the serial EKF with the experimental RSS measurements and simulated acceleration data is shown. The RMSE value of the ONLY RSS case is 1.93 m where the sensor fusion decreased the error to 1.54 m. Parallel EKF performance is also shown in Figure 5.10 and the RMSE values are 1.78 m and 1.52 m for ONLY RSS and sensor fusion respectively. Lastly, KF is executed to estimate trajectory of the blindfolded node and results are presented in Figure 5.11. The RMSE values are 2.04 m and 1.85 m for the ONLY RSS and RSS/IMU fusion cases respectively.
- As a conclusion, static localization performance can be enhanced the tracking filters to reach accuracy 1 m and sensor fusion decreases the the error approximately by 15% experimentally.

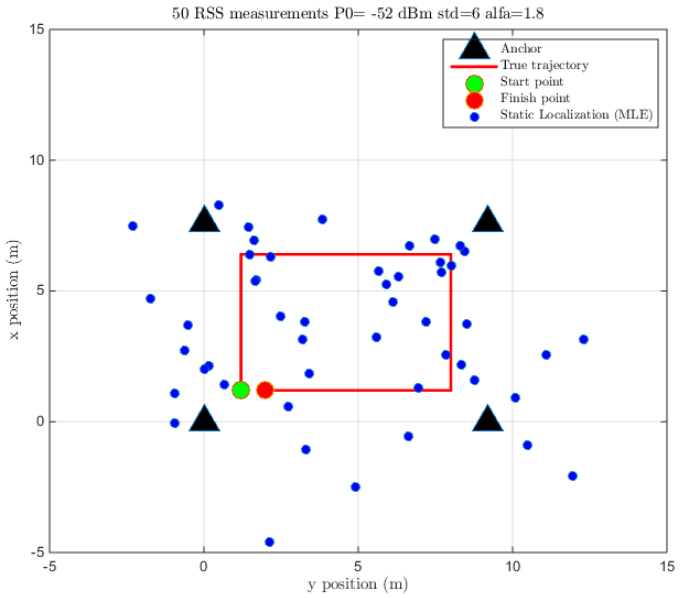

Figure 5.8: Estimated static locations from the RSS observations by using MLE, P_0 = -52 dBm , σ_{RSS} = 6 dB , α = 1.8

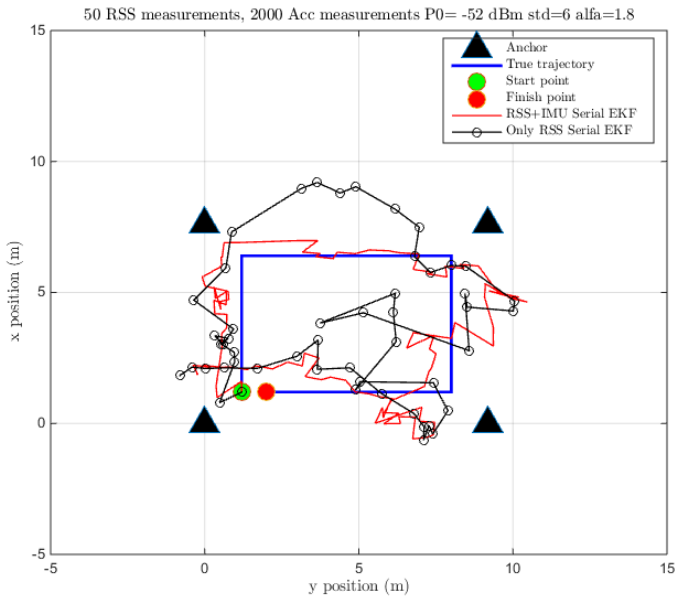

Figure 5.9: Performance of the Serial EKF for the both ONLY RSS and RSS/IMU fusion cases with the experimental RSS measurements and simulated acceleration measurements, P_0 = -52 dBm , σ_{RSS} = 6 dB , α = 1.8

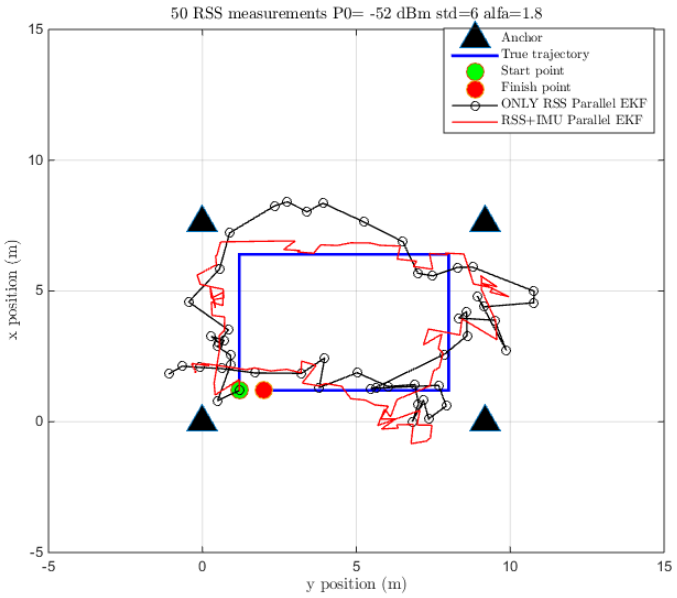

Figure 5.10: Performance of the Parallel EKF for the both ONLY RSS and RSS/IMU fusion cases with the experimental RSS measurements and simulated acceleration measurements, P_0 = -52 dBm , σ_{RSS} = 6 dB , α = 1.8

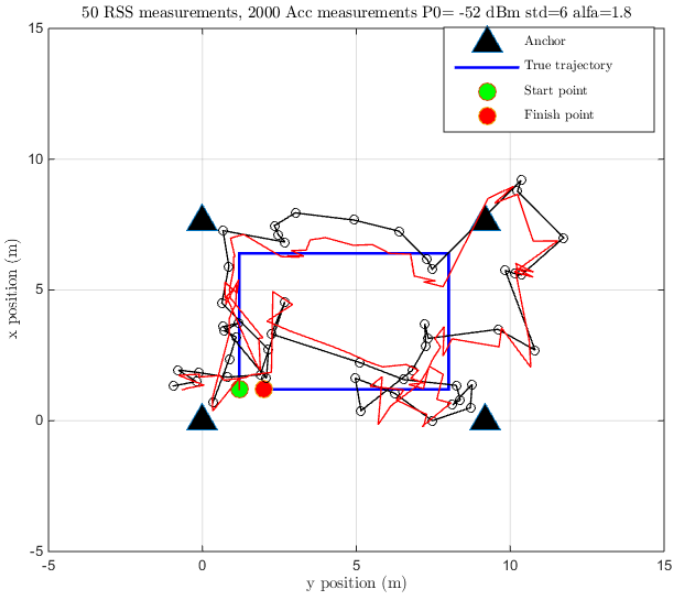

Figure 5.11: Performance of the KF for the both ONLY RSS and RSS/IMU fusion cases with the experimental RSS measurements and simulated acceleration measurements, P_0 = -52 dBm , σ_{RSS} = 6 dB , α = 1.8

CHAPTER 6

CONCLUSION

In this thesis, we first studied the performance of the RSS based localization and tracking algorithms (MLE, KF, Serial EKF, Parallel EKF) for indoor environments in WSN through various simulations. It has been shown that tracking enhances the accuracy of static localization and processing the RSS measurements serially (Serial EKF) gives a little advantage.

Later, we discussed the RSS/IMU sensor fusion for target tracking to improve accuracy of RSS based tracking by using EKF and KF as fusion algorithms. In the proposed method, position estimation starts with the raw acceleration data and whenever an RSS measurement is available, estimated location is updated. It was observed that sensor fusion scheme mitigates the effects of fluctuations from RSSI and overcomes the drift problem from the IMU. The average performance enhancement of tracking by sensor fusion is around 30%. Channel parameters and IMU precision are key parameters and they deeply affect the estimated trajectory. It is shown that 1 meter RMSE is reachable with RSS measurements under the condition that variance of RSS is 3 dB. Decreasing the accelerometer noise standard deviation to 0.0075 m/s^2 also pulls down the fusion case's error below 1 meter.

The derivation of a theoretical bound in terms of MSE for a single target tracking in WSN was investigated for the ONLY RSS and RSS/IMU fusion scenarios in Chapter 4. A nearly constant acceleration model was used and an approximation to the posterior Cramer-Rao Bound was derived by sequential Monte Carlo integration for non-linear measurement model of RSS. Since the channel parameters, sensor precision and posterior density of the state are key factors in the derivation of the bound, we

compared PCRLBs for several RSS and accelerometer noise variances. This PCRLB can be used as a benchmark for channel and sensor selection in target tracking applications.

Finally, WSN and testbed are implemented by using Xbee S2 RF modules and Arduino Uno R3 boards to experimentally investigate tracking algorithms. Channel parameters were estimated in the calibration phase yet it was observed that different PLE gave better performance rather than the estimated one. It has been experimentally observed that filters surpass the performance of localization in the sense of RMSE. In addition, sensor fusion scheme decreases the error approximately 15%. Also variation of RSS values with respect to antenna type and orientation is discussed in Chapter 5. Radiation pattern of the chip antenna is not isotropic and antenna orientation has a great impact on RSS.

As a future work, comparison of sensor fusion and only RSS scenarios may be done experimentally with the proper IMU and RF modules. Also estimating channel parameters dynamically and refinement of movement models by target orientation estimation from the IMU (gyroscope, magnetometer and acceleration) can be examined to increase tracking accuracy. Sensor selection algorithms can be implemented for different data sources by using the PCRLB for indoor positioning systems.

REFERENCES

[1] Umut Orguner. Ee793 target tracking: Lecture 1 introduction to state estimation. `http://www.eee.metu.edu.tr/~umut/ee793/files/METULecture1.pdf`. [Last accessed on November 2015].

[2] Cauligi S Raghavendra, Krishna M Sivalingam, and Taieb Znati. *Wireless sensor networks*. Springer, 2006.

[3] Elliott Kaplan and Christopher Hegarty. *Understanding GPS: principles and applications*. Artech house, 2005.

[4] Amitangshu Pal. Localization algorithms in wireless sensor networks: Current approaches and future challenges. *Network Protocols and Algorithms*, 2(1):45–73, 2010.

[5] Yanying Gu, Anthony Lo, and Ignas Niemegeers. A survey of indoor positioning systems for wireless personal networks. *Communications Surveys & Tutorials, IEEE*, 11(1):13–32, 2009.

[6] Xinrong Li. Collaborative localization with received-signal strength in wireless sensor networks. *Vehicular Technology, IEEE Transactions on*, 56(6):3807–3817, 2007.

[7] Neal Patwari, Alfred O Hero III, Matt Perkins, Neiyer S Correal, and Robert J O'dea. Relative location estimation in wireless sensor networks. *Signal Processing, IEEE Transactions on*, 51(8):2137–2148, 2003.

[8] Yi Shang, Wheeler Ruml, Ying Zhang, and Markus PJ Fromherz. Localization from mere connectivity. In *Proceedings of the 4th ACM international symposium on Mobile ad hoc networking & computing*, pages 201–212. ACM, 2003.

[9] Zheng Yang and Yunhao Liu. Quality of trilateration: Confidence-based iterative localization. *Parallel and Distributed Systems, IEEE Transactions on*, 21(5):631–640, 2010.

[10] Andreas Savvides, Heemin Park, and Mani B Srivastava. The bits and flops of the n-hop multilateration primitive for node localization problems. In *Proceedings of the 1st ACM international workshop on Wireless sensor networks and applications*, pages 112–121. ACM, 2002.

[11] Francois Caron, Emmanuel Duflos, Denis Pomorski, and Philippe Vanheeghe. GPS/IMU data fusion using multisensor Kalman filtering: introduction of contextual aspects. *Information Fusion*, 7(2):221–230, 2006.

[12] Veerachai Malyavej, Warapon Kumkeaw, and Manop Aorpimai. Indoor robot localization by rssi/imu sensor fusion. In *Electrical Engineering/Electronics, Computer, Telecommunications and Information Technology (ECTI-CON), 2013 10th International Conference on*, pages 1–6. IEEE, 2013.

[13] William Wei-Liang Li, Ronald Iltis, Moe Z Win, et al. A smartphone localization algorithm using RSSI and inertial sensor measurement fusion. In *Global Communications Conference (GLOBECOM), 2013 IEEE*, pages 3335–3340. IEEE, 2013.

[14] Julian Lategahn, Marcel Müller, and Christof Röhrig. Robust pedestrian localization in indoor environments with an IMU aided TDoA system. In *Proceedings of the 5th International Conference on Indoor Positioning and Indoor Navigation*, 2014.

[15] Rong Peng and Mihail L Sichitiu. Angle of arrival localization for wireless sensor networks. In *Sensor and Ad Hoc Communications and Networks, 2006. SECON'06. 2006 3rd Annual IEEE Communications Society on*, volume 1, pages 374–382. IEEE, 2006.

[16] Dragos Niculescu and Badri Nath. Ad hoc positioning system (APS) using AOA. In *INFOCOM 2003. Twenty-Second Annual Joint Conference of the IEEE Computer and Communications. IEEE Societies*, volume 3, pages 1734–1743. IEEE, 2003.

[17] Andrea Goldsmith. *Wireless communications*. Cambridge university press, 2005.

[18] Neal Patwari, R Dea, and Yanwei Wang. Relative location in wireless networks. In *Vehicular Technology Conference, 2001. VTC 2001 Spring. IEEE VTS 53rd*, volume 2, pages 1149–1153. IEEE, 2001.

[19] Neal Patwari. *Location estimation in sensor networks*. PhD thesis, The University of Michigan, 2005.

[20] Ingwer Borg and Patrick JF Groenen. *Modern multidimensional scaling: Theory and applications*. Springer Science & Business Media, 2005.

[21] Guoqiang Mao, Barış Fidan, and Brian DO Anderson. Wireless sensor network localization techniques. *Computer networks*, 51(10):2529–2553, 2007.

[22] Avanthi Koneru, Xinrong Li, and Murali Varanasi. Comparative study of RSS-based collaborative localization methods in sensor networks. In *Region 5 Conference, 2006 IEEE*, pages 243–248. IEEE, 2006.

[23] Eunchan Kim, Sangho Lee, Chungsan Kim, and Kiseon Kim. Mobile beacon-based 3d-localization with multidimensional scaling in large sensor networks. *Communications Letters, IEEE*, 14(7):647–649, 2010.

[24] Jan De Leeuw and Patrick Mair. Multidimensional scaling using majorization: Smacof in r. *Department of Statistics, UCLA*, 2011.

[25] Labyad Asmaa, Kharraz Aroussi Hatim, and Mouloudi Abdelaaziz. Localization algorithms research in wireless sensor network based on multilateration and trilateration techniques. In *Information Science and Technology (CIST), 2014 Third IEEE International Colloquium in*, pages 415–419. IEEE, 2014.

[26] Andreas Savvides, Chih-Chieh Han, and Mani B Strivastava. Dynamic fine-grained localization in ad-hoc networks of sensors. In *Proceedings of the 7th annual international conference on Mobile computing and networking*, pages 166–179. ACM, 2001.

[27] Sudha Challa. *Fundamentals of object tracking*. Cambridge University Press, 2011.

[28] Brian DO Anderson and John B Moore. *Optimal filtering*. Courier Corporation, 2012.

[29] Neil Gordon, B Ristic, and S Arulampalam. Beyond the Kalman filter: Particle filters for tracking applications. *Artech House, London*, 2004.

[30] Andrew H Jazwinski. *Stochastic processes and filtering theory*. Courier Corporation, 2007.

[31] Jianye Ching, James L Beck, and Keith A Porter. Bayesian state and parameter estimation of uncertain dynamical systems. *Probabilistic engineering mechanics*, 21(1):81–96, 2006.

[32] Rudolph Emil Kalman. A new approach to linear filtering and prediction problems. *Journal of Fluids Engineering*, 82(1):35–45, 1960.

[33] Peter S Maybeck. *Stochastic models, estimation, and control*, volume 3. Academic press, 1982.

[34] Fredrik Gustafsson. Statistical sensor fusion. 2010.

[35] Eric Wan, Ronell Van Der Merwe, et al. The unscented Kalman filter for nonlinear estimation. In *Adaptive Systems for Signal Processing, Communications, and Control Symposium 2000. AS-SPCC. The IEEE 2000*, pages 153–158. IEEE, 2000.

[36] Simon J Julier and Jeffrey K Uhlmann. Unscented filtering and nonlinear estimation. *Proceedings of the IEEE*, 92(3):401–422, 2004.

[37] Sanjoy K Mitter. *Approximations for nonlinear filtering*. Springer, 1983.

[38] Harold J Kushner. Approximations to optimal nonlinear filters. *Automatic Control, IEEE Transactions on*, 12(5):546–556, 1967.

[39] Harold W SORENSON and Allen R STUBBERUD. Non-linear filtering by approximation of the a posteriori density. *International Journal of Control*, 8(1):33–51, 1968.

[40] Simon J Julier and Jeffrey K Uhlmann. New extension of the kalman filter to nonlinear systems. In *AeroSense'97*, pages 182–193. International Society for Optics and Photonics, 1997.

[41] Veerachai Malyavej and Prakasit Udomthanatheera. RSSI/IMU sensor fusion-based localization using unscented kalman filter. *Communications (APCC), 2014 Asia-Pacific Conference on*, pages 227–232, 2014.

[42] JD Hol. *Sensor Fusion and Calibration using Inertial Sensors, Vision, Ultra-Wideband and GPS*. PhD thesis, Linköping University, Division of Automatic Control, 2011.

[43] Yogita Chapre, Prasant Mohapatra, Somesh Jha, and Aruna Seneviratne. Received signal strength indicator and its analysis in a typical WLAN system (short paper). In *Local Computer Networks (LCN), 2013 IEEE 38th Conference on*, pages 304–307. IEEE, 2013.

[44] Harry L Van Trees. *Detection, estimation, and modulation theory*. John Wiley & Sons, 2004.

[45] Petr Tichavskỳ, Carlos H Muravchik, and Arye Nehorai. Posterior Cramér-Rao bounds for discrete-time nonlinear filtering. *Signal Processing, IEEE Transactions on*, 46(5):1386–1396, 1998.

[46] `http://www.digi.com/products/xbee-rf-solutions/modules/xbee-zigbee`. [Last accessed November 2015].

[47] Wideband millimeter-wave propagation measurements and channel models for future wireless communication system design. *IEEE Transactions on Communications*, 63(9):3029–3056, 2015.

[48] Meriç Koray Karakurt. An experimental investigation on indoor RSSI-based localization. Master's thesis, Middle East Technical University, 2013.

[49] PJM Havinga et al. RSS-based localization with different antenna orientations. In *Telecommunication Networks and Applications Conference (ATNAC), 2010 Australasian*, pages 13–18. IEEE, 2010.

[50] Cc2430 datasheet. `http://www.ti.com/lit/ds/symlink/cc2430.pdf`. [Last accessed on November 2015].